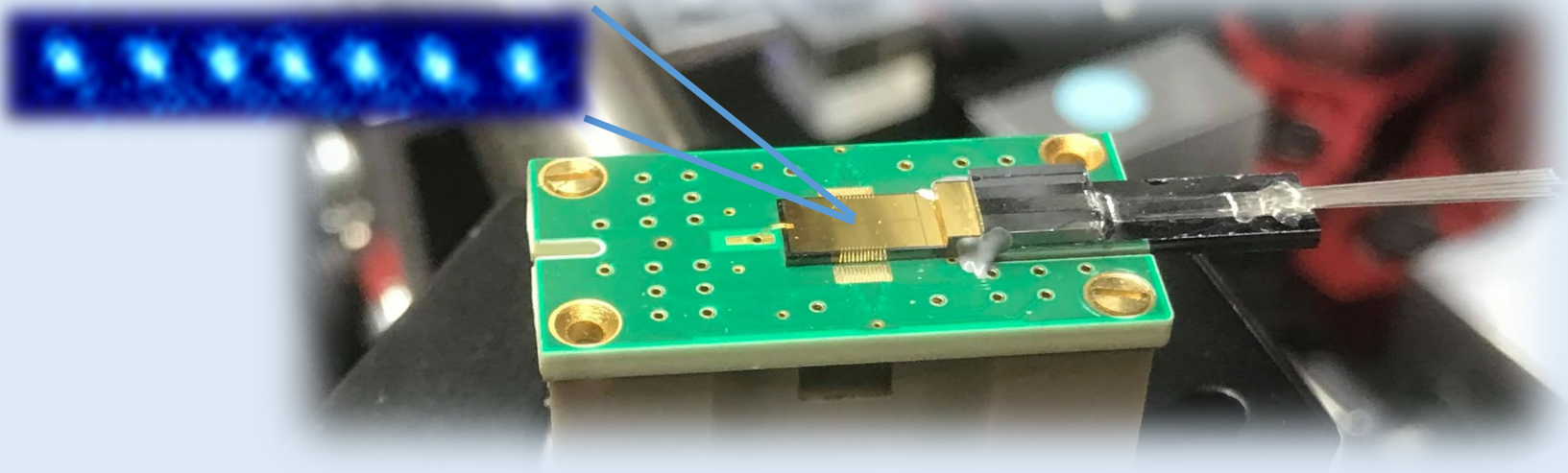
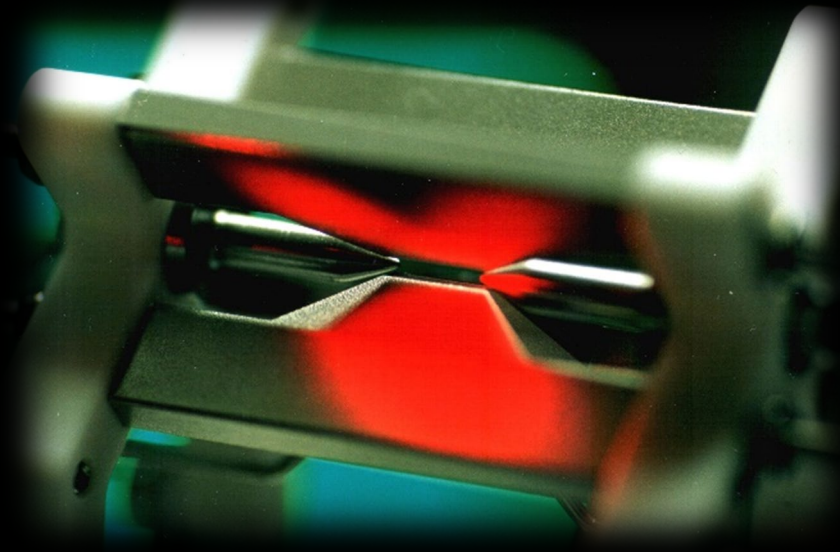


Quantum computing with trapped ions

Jonathan Home
Institute for Quantum Electronics, ETH Zürich



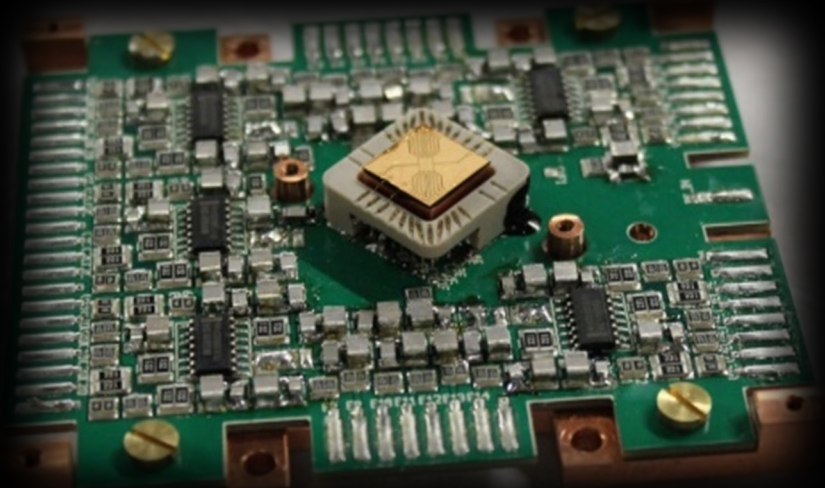
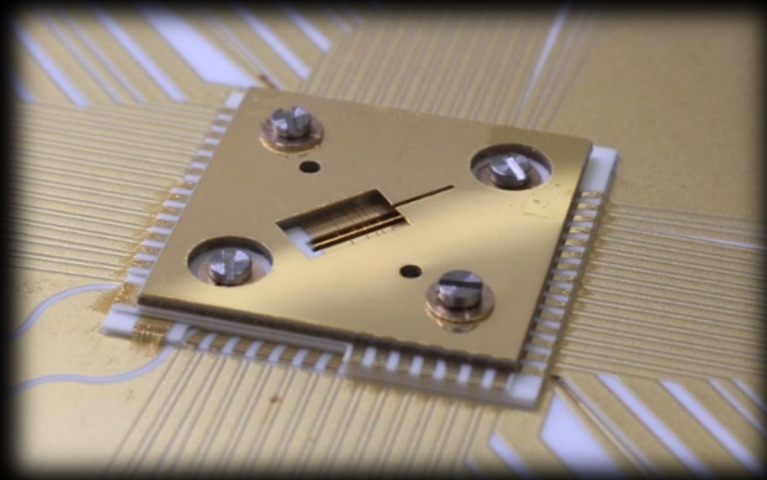
Trapped ions



Room temperature

$$V_{\text{static}}(\mathbf{r}) + \Phi_{\text{RF}}(\mathbf{r})$$

Ponderomotive potential
(change of rapid kinetic motion with position)




4 Kelvin

Radio-frequency ion traps

Laplace's equation

– no chance to trap with static fields

$$\frac{\partial^2 V}{\partial x^2} + \frac{\partial^2 V}{\partial y^2} + \frac{\partial^2 V}{\partial z^2} = 0$$


Paul trap: Use a ponderomotive potential – change potential fast compared to speed of ion

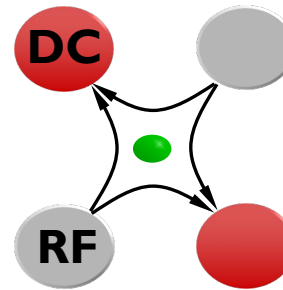
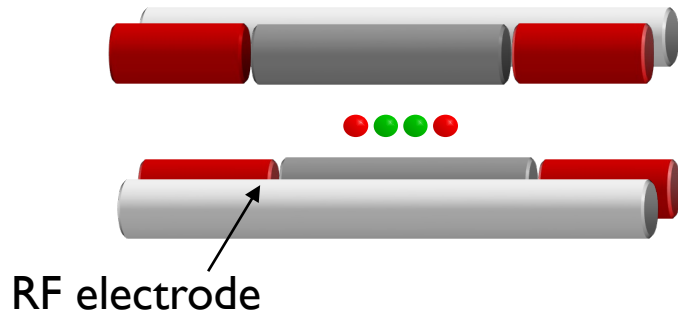
$$\frac{\partial^2 V}{\partial x^2} + \left(\frac{\partial^2 V}{\partial y^2} + \frac{\partial^2 V}{\partial z^2} \right) \cos(\Omega t)$$

$$M \frac{d^2 x}{dt^2} = qE \cos \Omega t \quad \frac{1}{2} M \left(\frac{dx}{dt} \right)^2 = U_{\text{PP}} = \frac{q^2 E^2}{2M\Omega^2} \sin^2 \Omega t$$

Time average - Effective potential energy which is minimal at minimum E

Penning trap: Add a homogeneous magnetic field – overrides the electric repulsion

The “workhorse” linear Paul trap

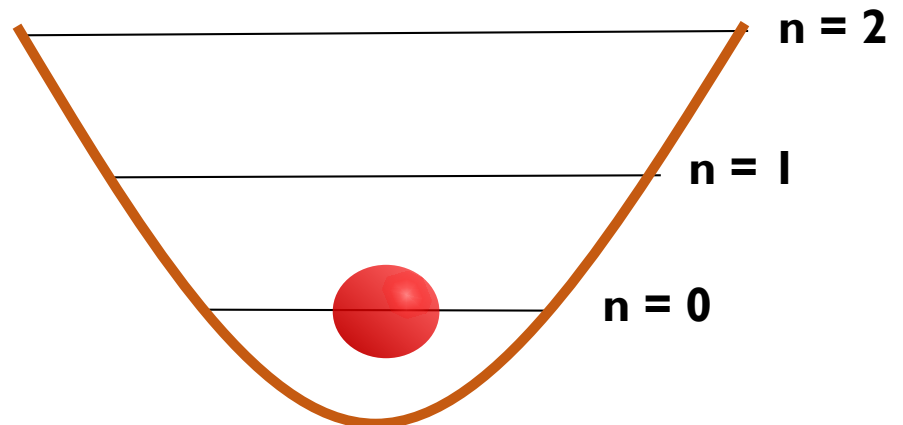


Trap Frequencies
Axial : < 3 MHz
Radial: < 20 MHz
Radial Freq $\propto 1/\text{Mass}$

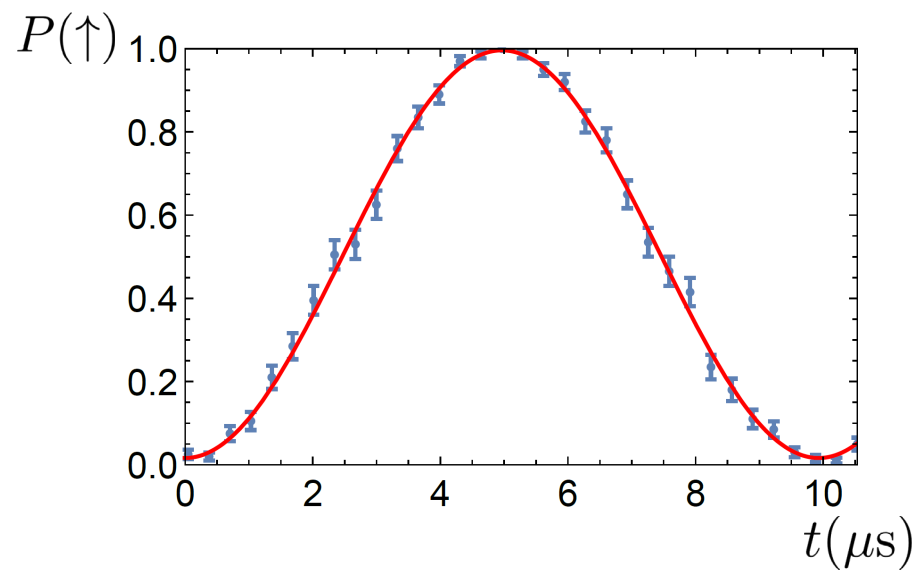
Potentials gives almost ideal harmonic behavior in 3D

Single ion

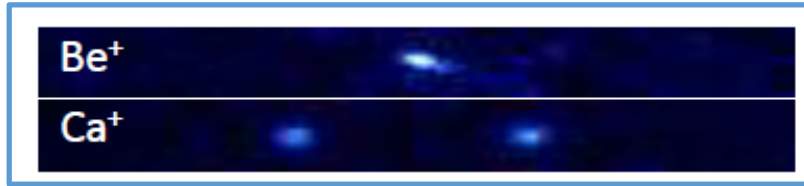
$$\hat{H} = \hbar\omega(\hat{a}^\dagger\hat{a} + 1/2)$$



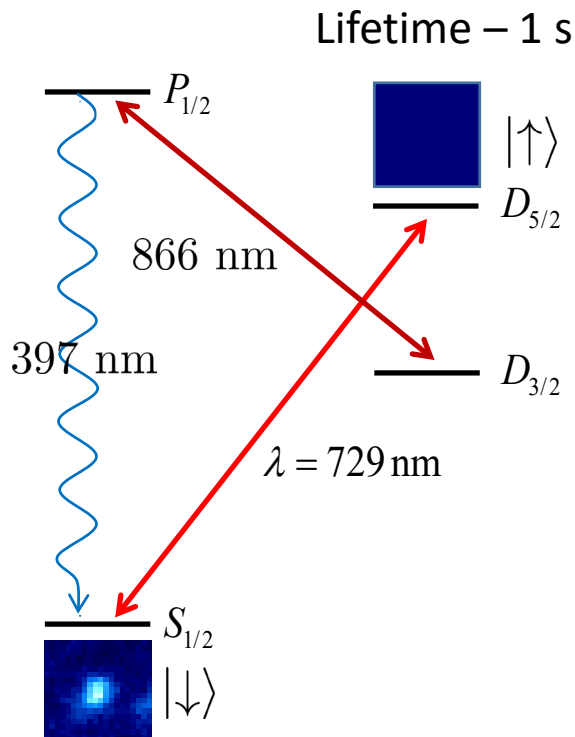
Internal state electronic qubits



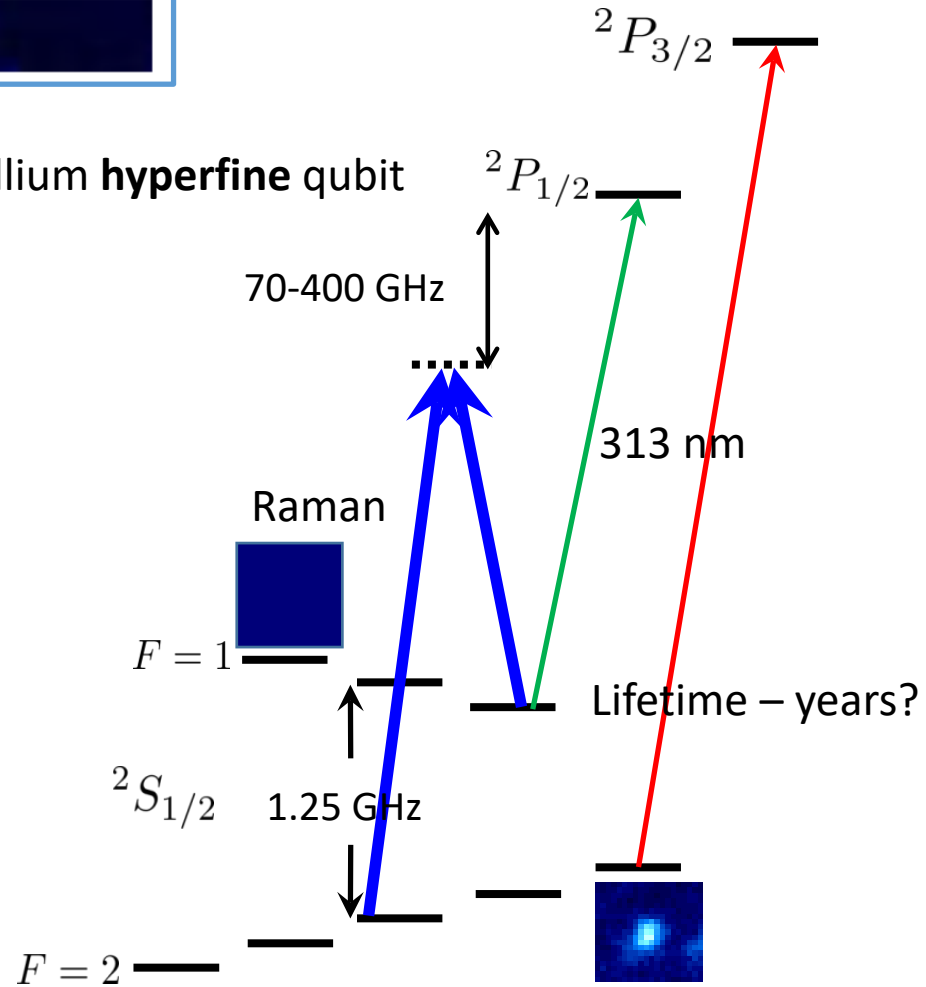
Qubit choices



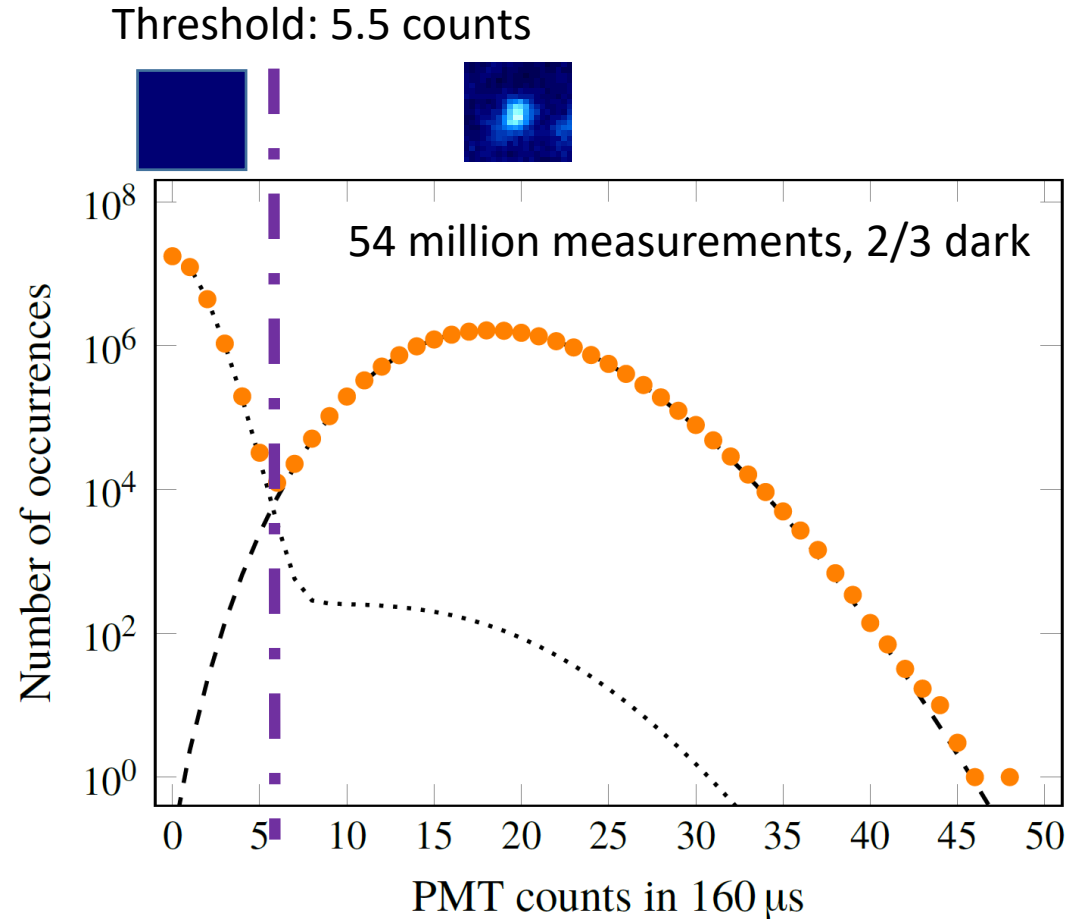
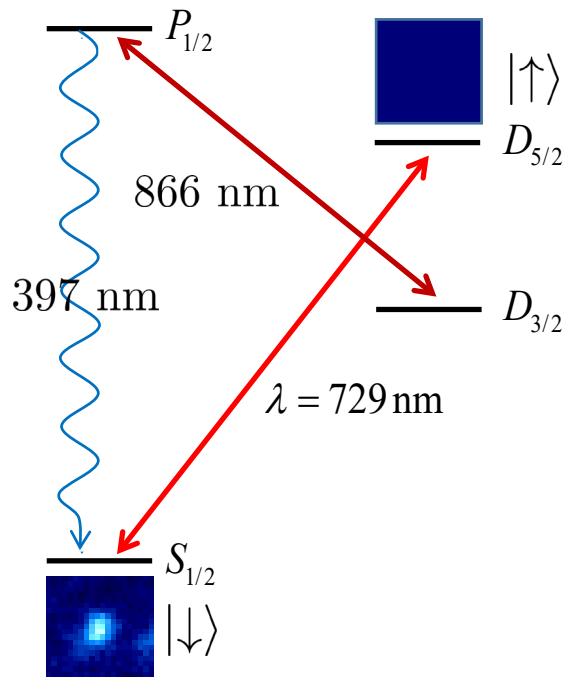
Calcium **optical** qubit



Beryllium **hyperfine** qubit



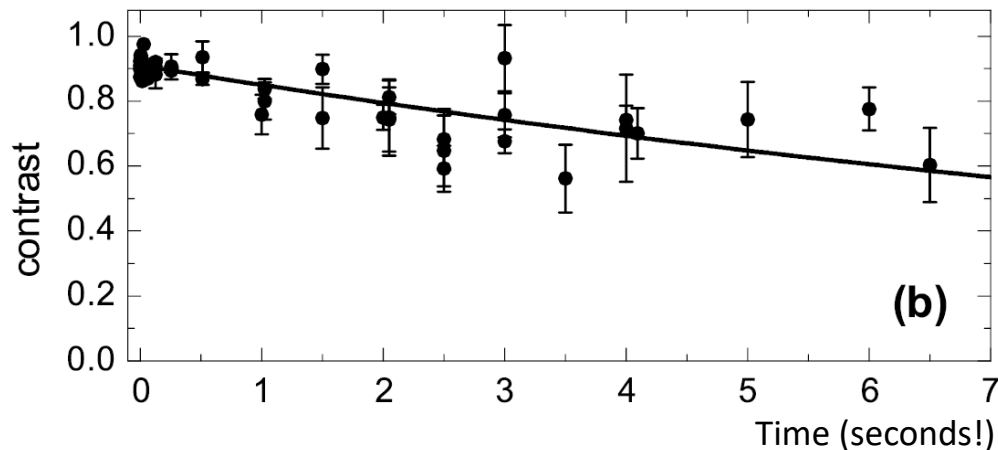
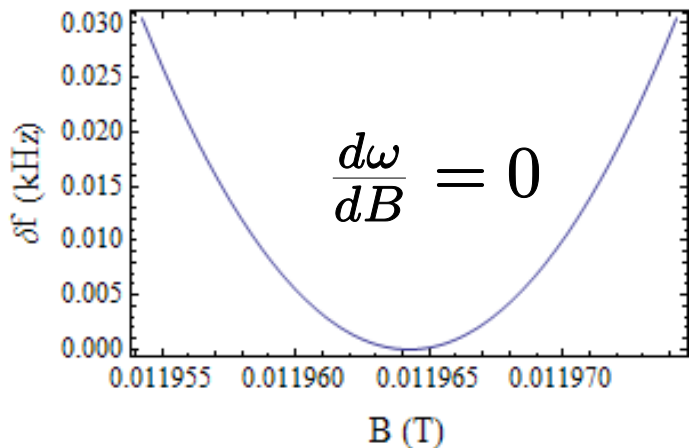
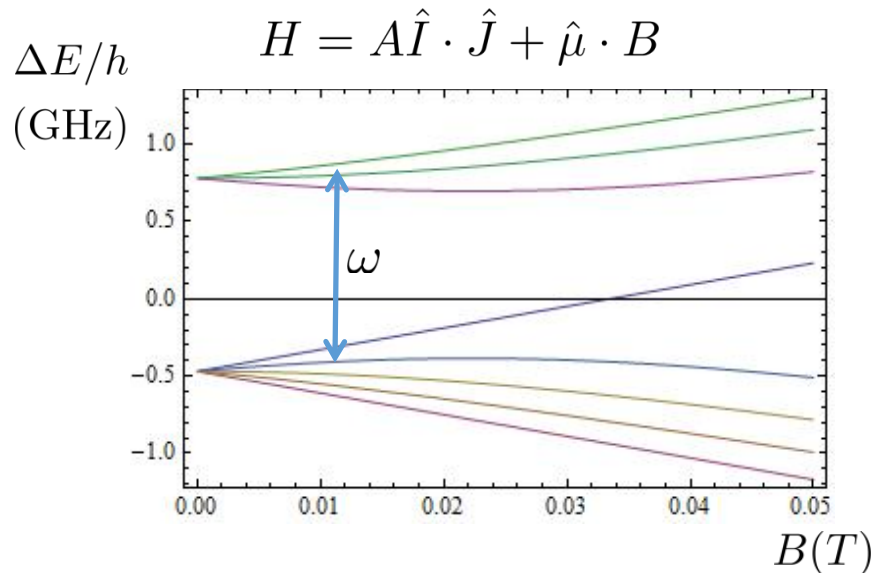
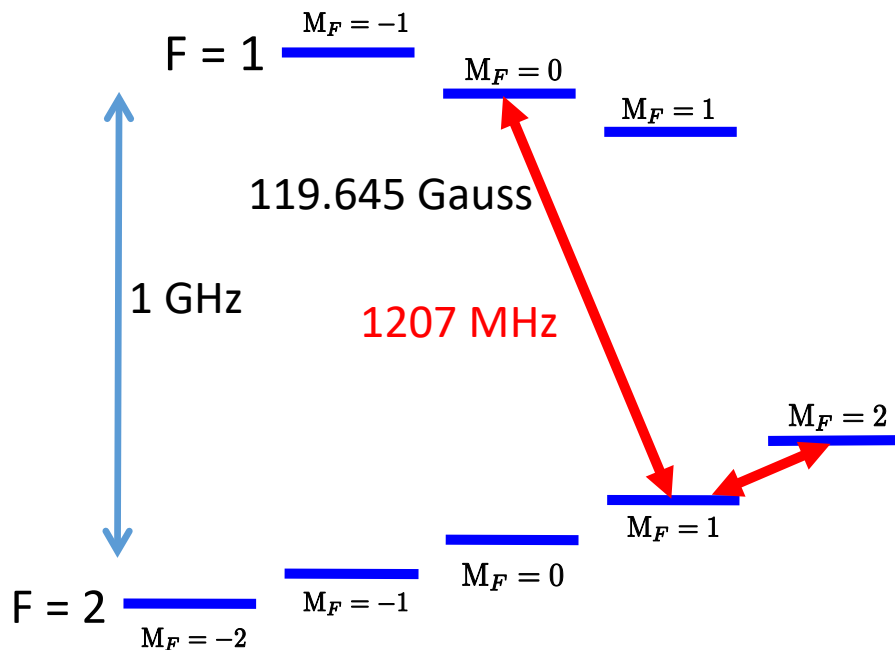
Qubit measurement



Single quantum system – many repeats
8,28,10,30,20,45,20 35

Single shot $p_{\text{error}} = 2 \times 10^{-4}$

Field-independent "clock" qubits



Identical qubits + Decoherence-Free Subspaces

Rejection of common-mode noise – DFS states for identical qubits

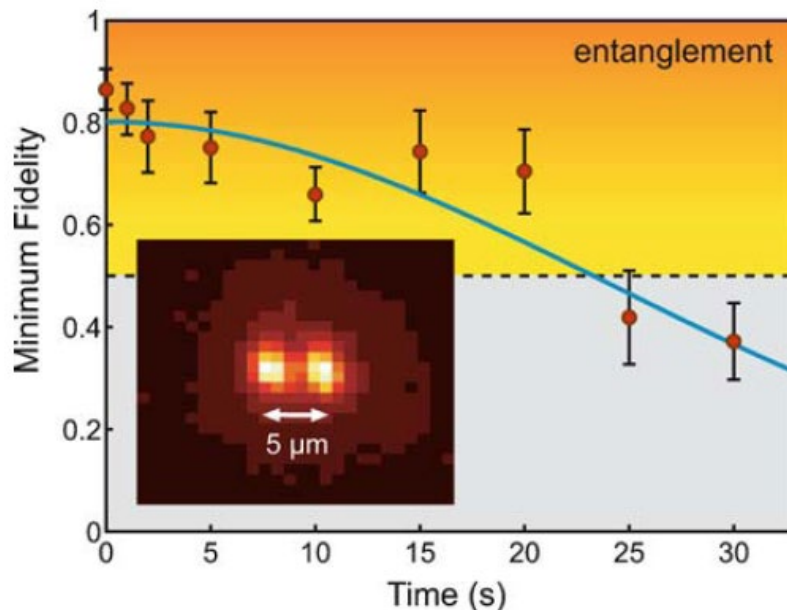
$$|0\rangle + e^{i\omega'(t)t} |1\rangle$$

$$|0\rangle + e^{i\omega(t)t} |1\rangle$$

Now consider entangled state

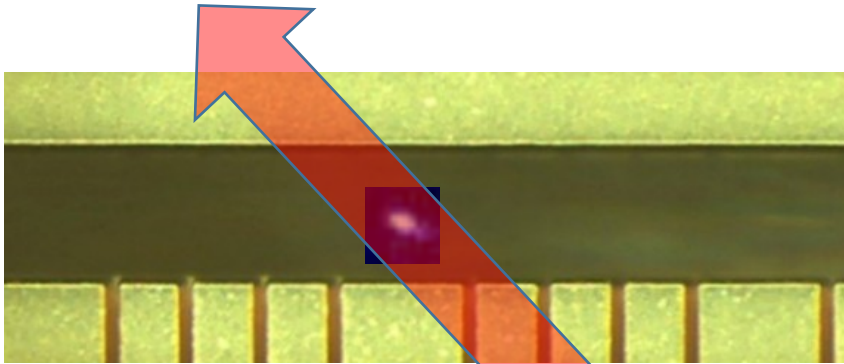
$$e^{i\omega(t)t} |01\rangle + e^{i\omega'(t)t} |10\rangle = e^{i\omega(t)t} \left(|01\rangle + e^{i(\omega'(t)-\omega(t))t} |10\rangle \right)$$

If noise is common mode, entangled states can have very long coherence times



Haffner et al., Appl. Phys. B 81, 151-153 (2005)

Single qubit gates – microwave or lasers



$I(t)$

$$\hat{H} = \begin{pmatrix} 0 & \Omega e^{i\phi} \\ \Omega e^{-i\phi} & 0 \end{pmatrix}$$

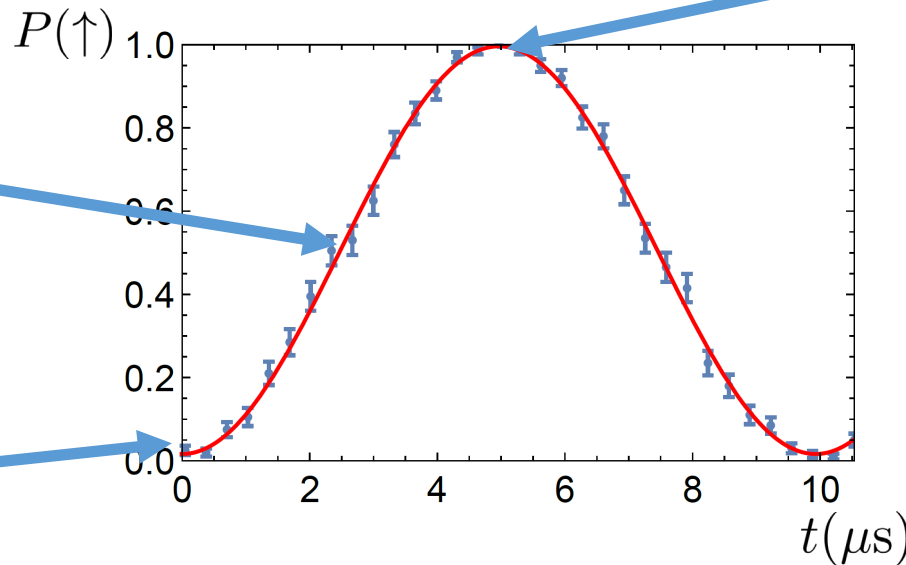
$$\hat{U}(t) = \cos(\theta/2)I + i \sin(\theta/2)\sigma_x$$

$$\theta = \Omega t$$

“Pi by two” pulse

$$\frac{1}{\sqrt{2}} (|\uparrow\rangle + e^{i\phi} |\downarrow\rangle)$$

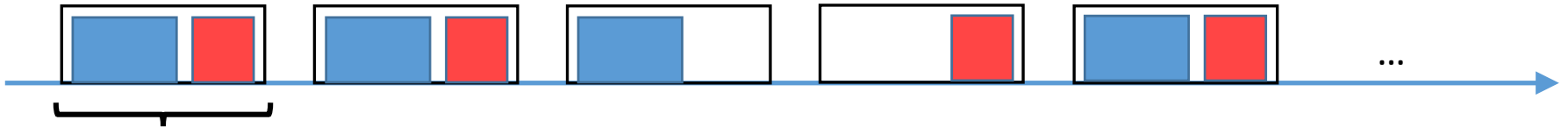
$|\downarrow\rangle$



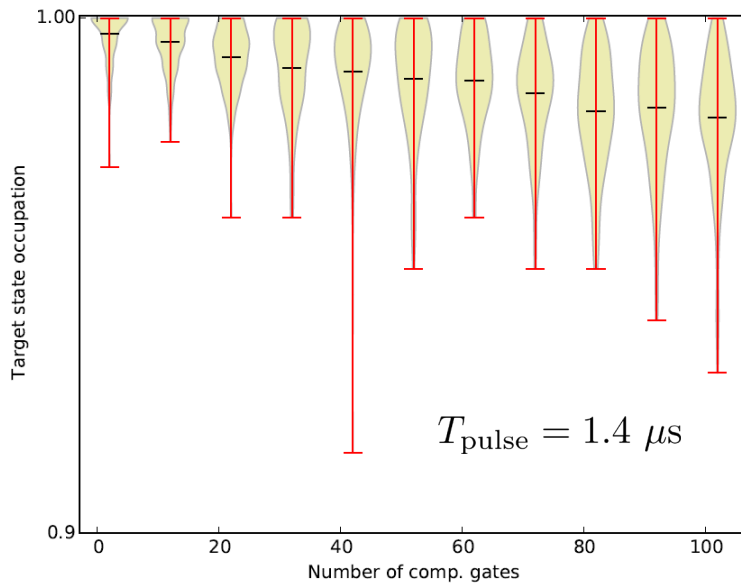
$|\uparrow\rangle$ “Pi” pulse

High fidelity single qubit gates

Method: Randomized benchmarking: long sequences of randomly chosen (known) operations



$$\text{Computational gate} = \hat{R}_j(\pi) \cdot \hat{R}_i(\pi/2) \quad i, j = \pm\hat{X}, \pm\hat{Y}, \pm\hat{Z}, \hat{I}$$

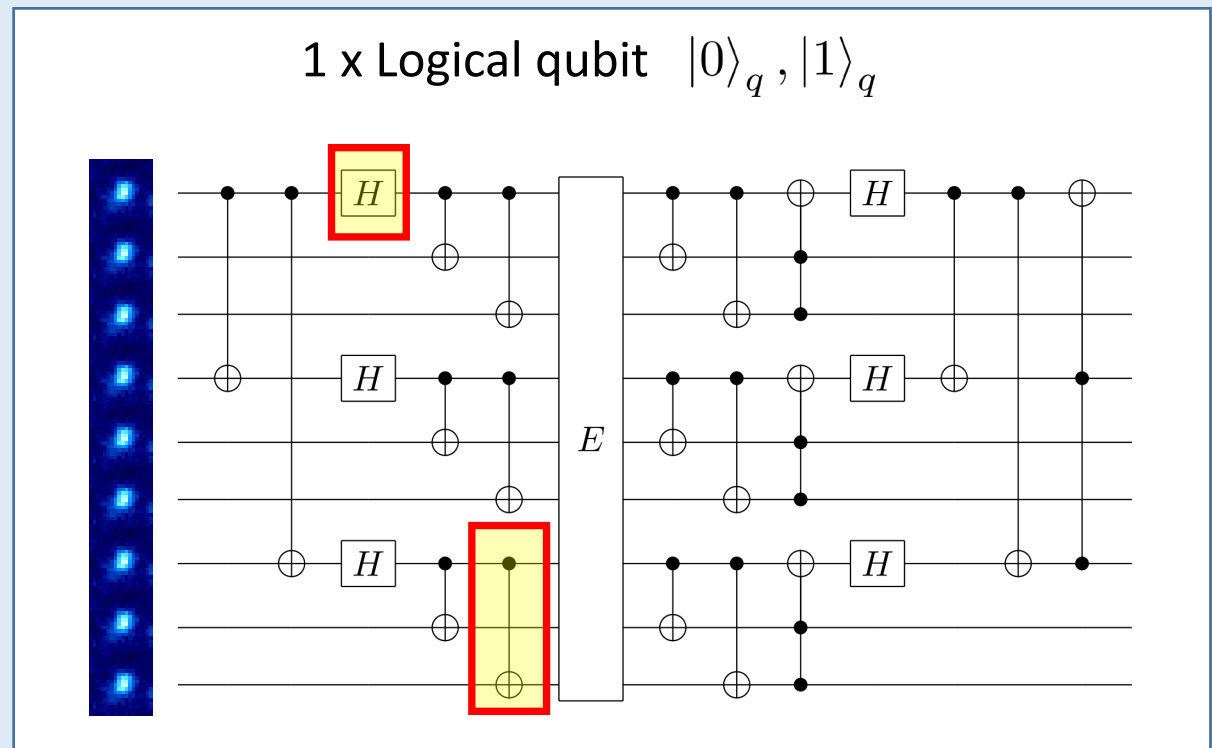


Average error > **99.98%** per computational gate

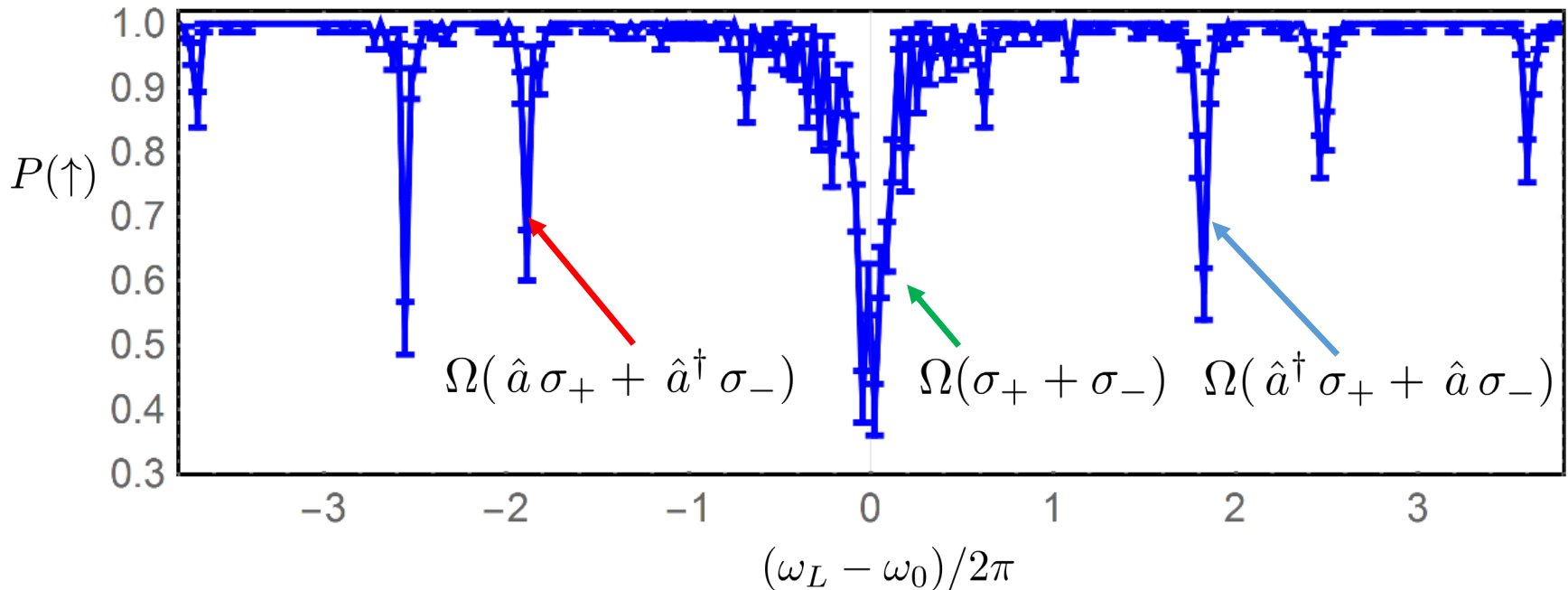
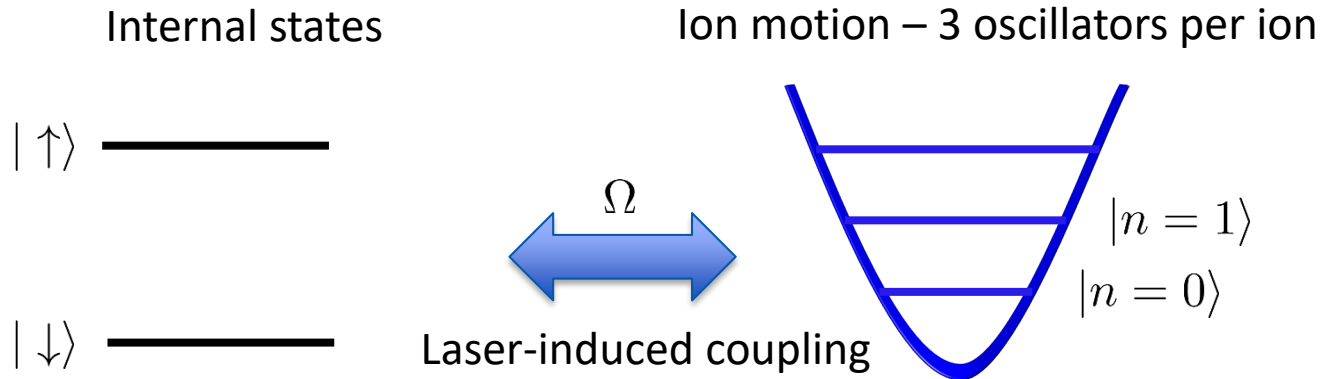
Highest fidelity operations: 0.999999 (Oxford, microwave drive)

Spin-spin interactions + multi-qubit gates

Realize circuits with *many* qubits

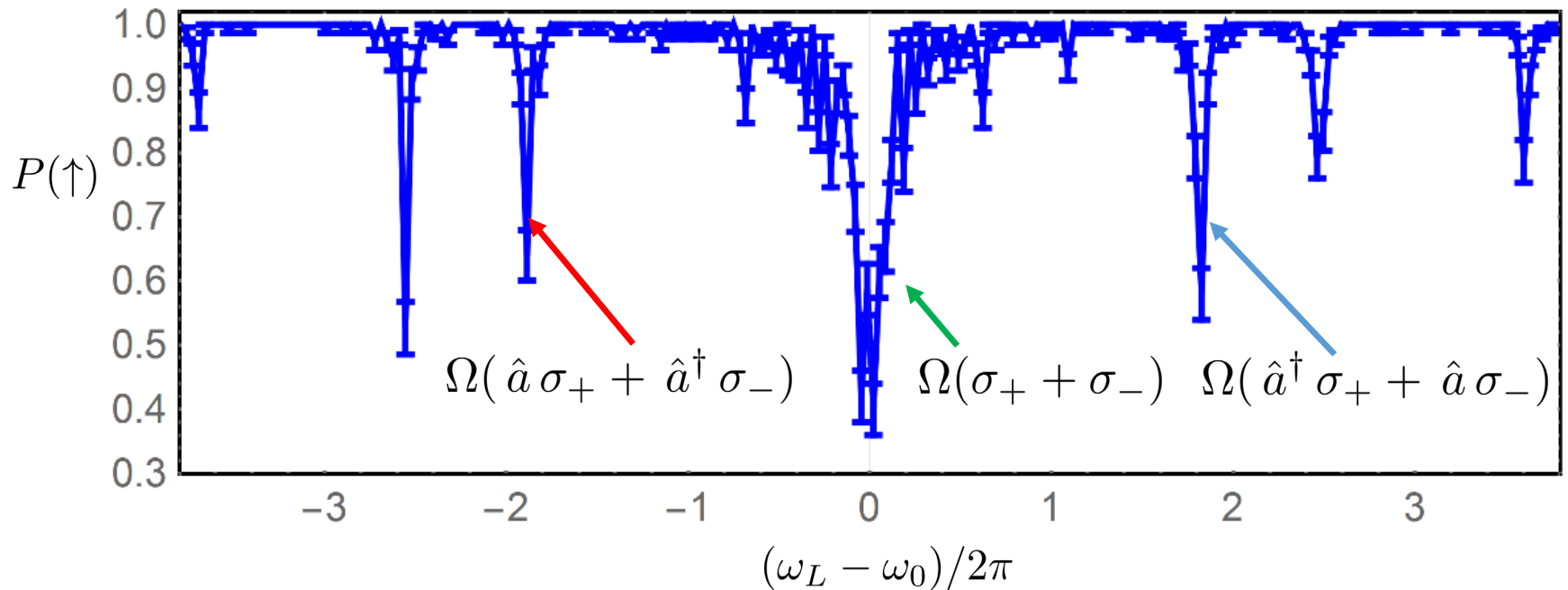
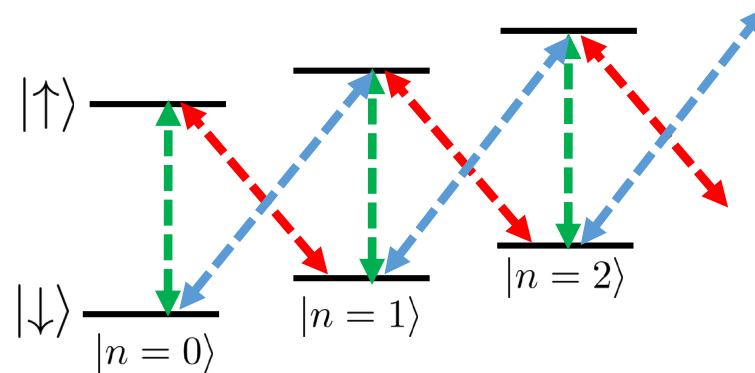


Parametrically coupled spin-oscillator system



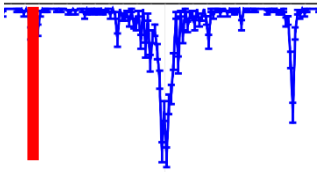
Choice of Hamiltonian

Laser frequency picks out resonant Hamiltonian

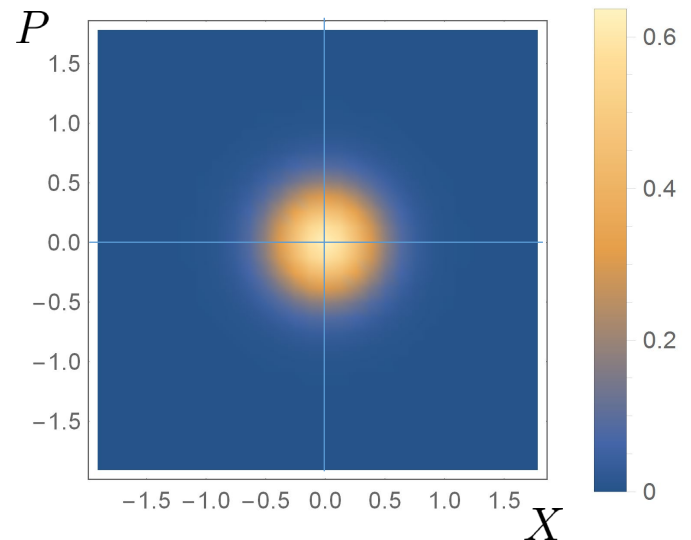
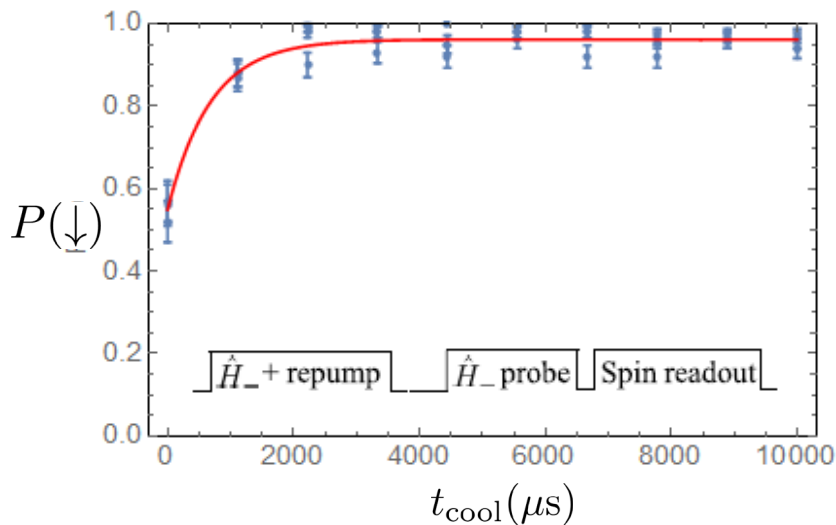
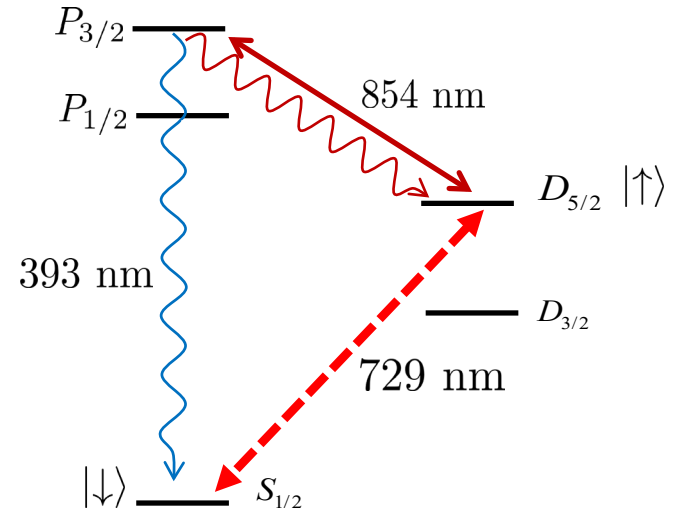
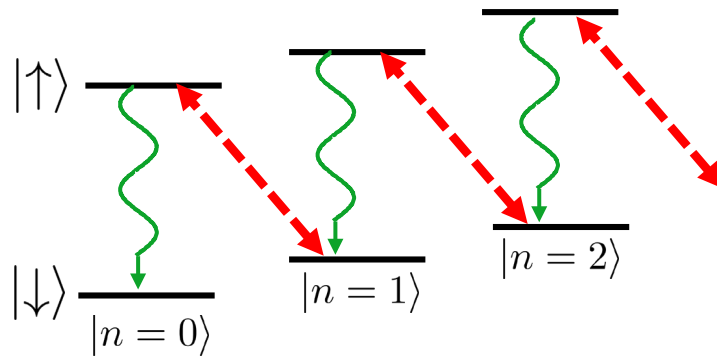


Ground state laser cooling

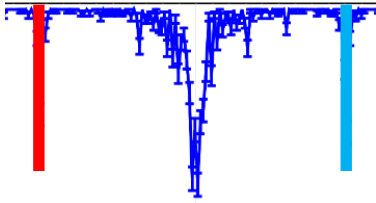
Monroe et al. PRL 75, 4011 (1995), Meekhof et al. PRL 76, 1796 (1996)



$$\hat{H}_r = \Omega(\hat{a} \sigma_+ + \hat{a}^\dagger \sigma_-)$$



Optical state-dependent force



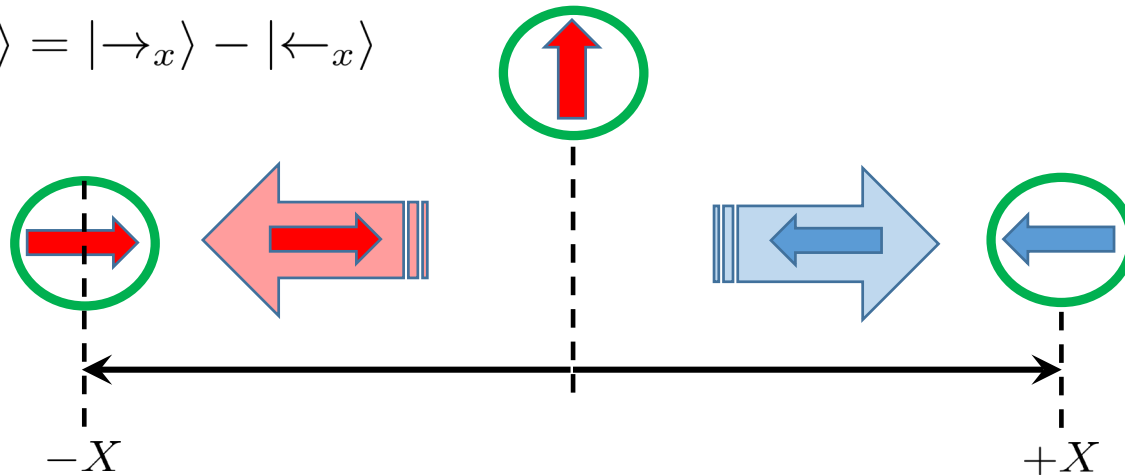
Equally driven resonant sidebands

$$\hat{H}_I = F_0 (\hat{a}^\dagger + \hat{a}) \sigma_x = F_0 X \sigma_x$$

$$U(t) = e^{-i \frac{F_0 t}{\hbar} X \sigma_x} = D(\alpha_X(t) \sigma_x)$$

Before

$$|\uparrow\rangle = |\rightarrow_x\rangle - |\leftarrow_x\rangle$$



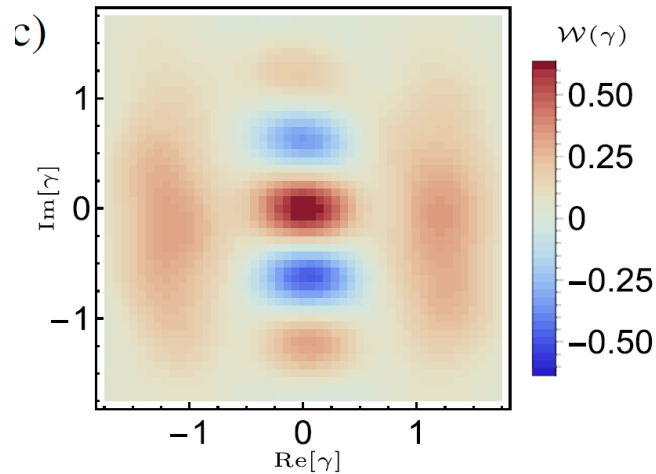
After

$$|\rightarrow\rangle |-\alpha_X\rangle + |\leftarrow\rangle |+\alpha_X\rangle$$

$$|\rightarrow\rangle \left| \begin{array}{c} \text{cat} \\ \uparrow \end{array} \right\rangle + |\leftarrow\rangle \left| \begin{array}{c} \text{cat} \\ \times \times \\ \uparrow \end{array} \right\rangle$$

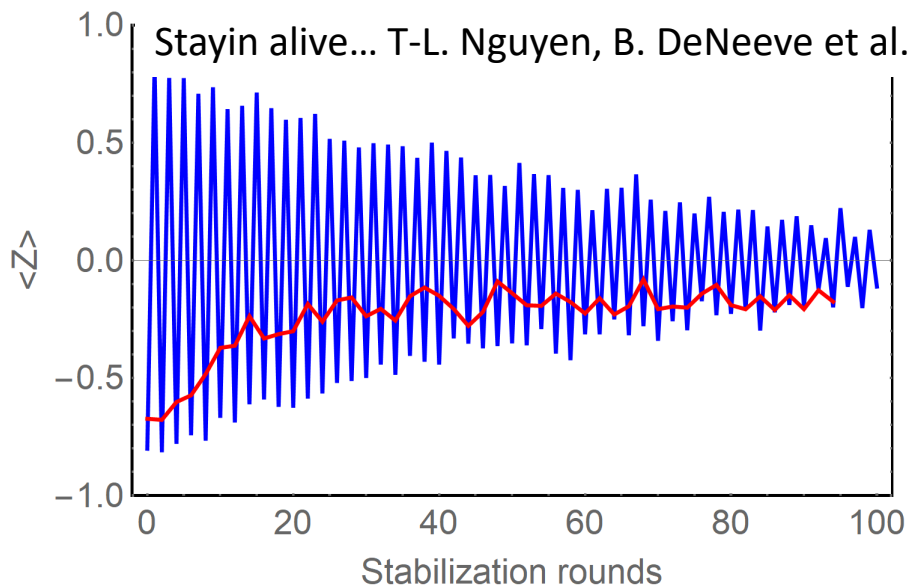
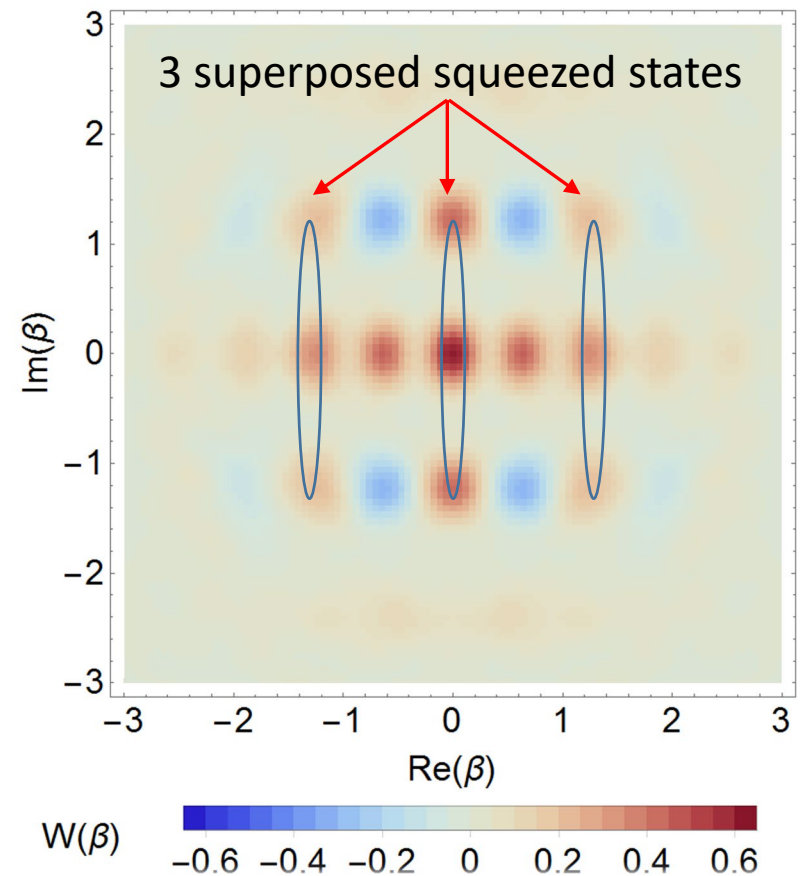
Cats which are squeezed, dead alive and in purgatory

C. Flühmann et al. PRL 125, 043602 (2020)

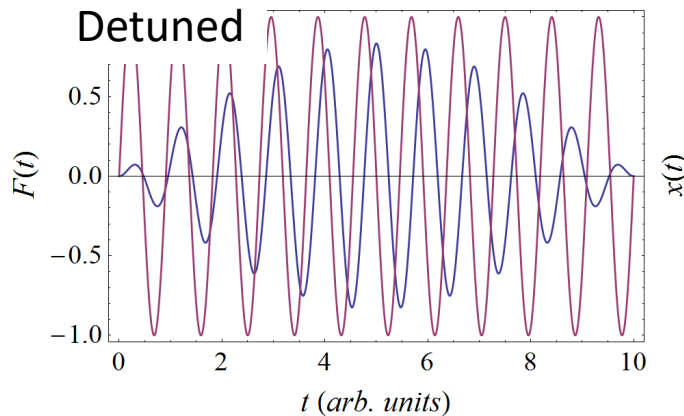
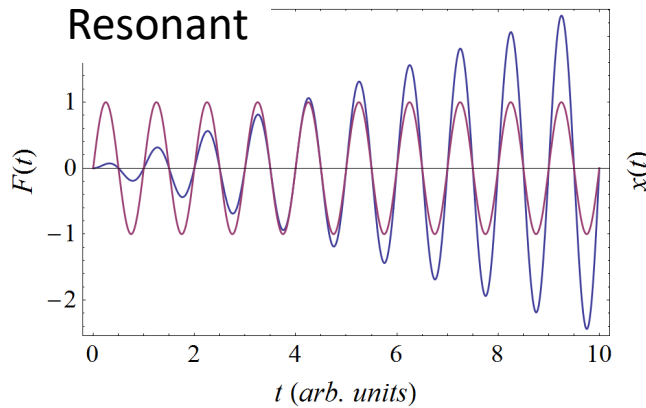


A quantum error-correction code

C. Flühmann et al. Nature 556, 513 (2019)



The forced harmonic oscillator



“returns” after

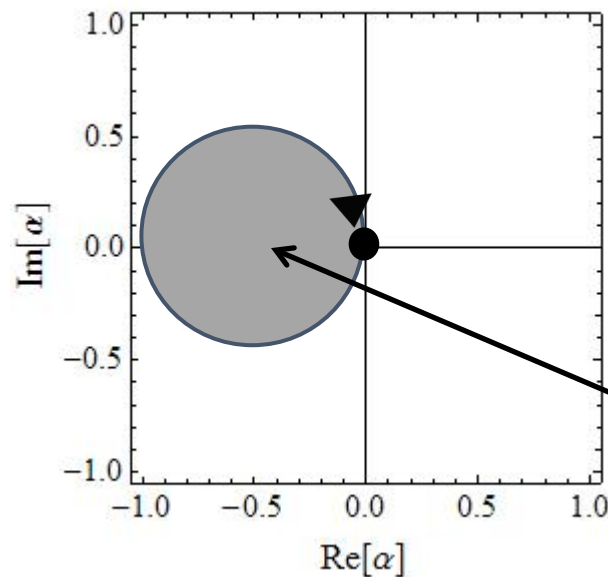
$$t = \frac{2\pi}{\delta}$$

Excitation amount

$$\propto \frac{F}{\delta}$$

Evolution
$$U = \exp \left(\frac{i}{\hbar} \int^t H(t') dt' - \frac{1}{2\hbar^2} \int^t \int^{t'} \underline{[H(t'), H(t'')] dt' dt''} + \dots \right)$$

Transient excitation,
phase acquired

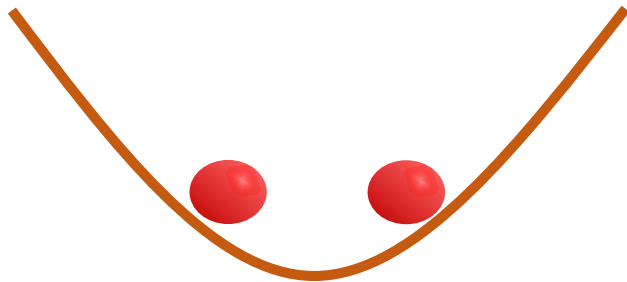


$$|1\rangle |\alpha_0\rangle \rightarrow e^{i\Phi} |1\rangle |\alpha_0\rangle$$

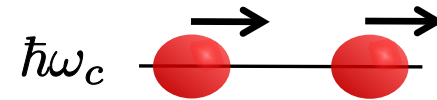
$$\Phi \propto A$$

State dependence and normal modes

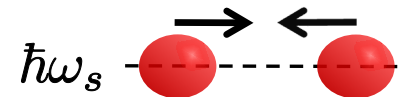
$$V = \frac{k}{2}z_1^2 + \frac{k}{2}z_2^2 + \frac{q^2}{4\pi\epsilon_0|z_1 - z_2|}$$



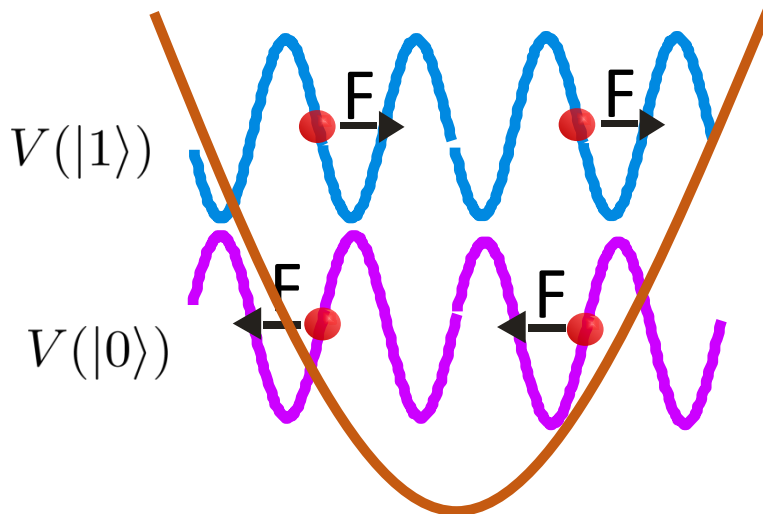
Independent normal mode oscillations
- shared motion



Stretch mode



Oscillating force close to resonance with **Stretch mode** of motion



$|1\rangle|1\rangle$

No Motion = no phase

$|1\rangle|0\rangle$

Motion = phase

$|0\rangle|1\rangle$

Motion = phase

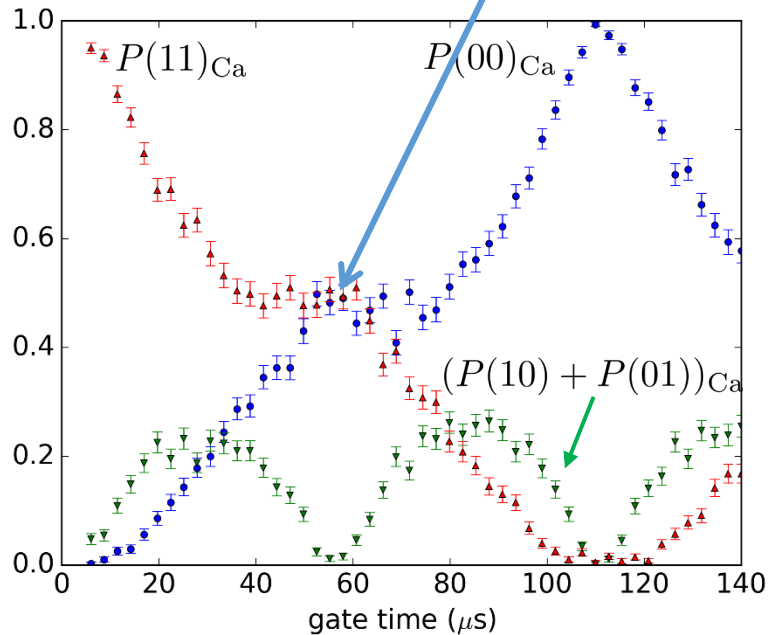
$|0\rangle|0\rangle$

No Motion = no phase

Gate time dynamics – 2 and 3 ions

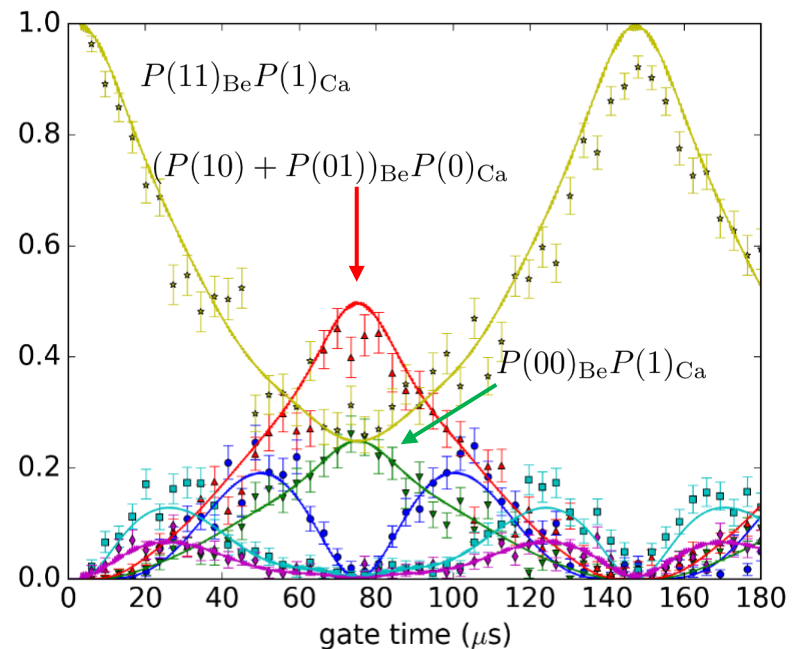
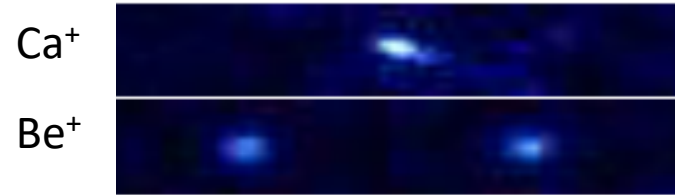
$$U(t) = D \left(\alpha(t) \hat{S}_x \right) e^{i\Phi(t) \hat{S}_x^2}$$

2 ions, 1 or 2 species $t = \frac{2\pi}{\delta_m}, \alpha(t) = 0$



Gate fidelities ~99 % (Be or Ca or both)

3 ions, 2 species



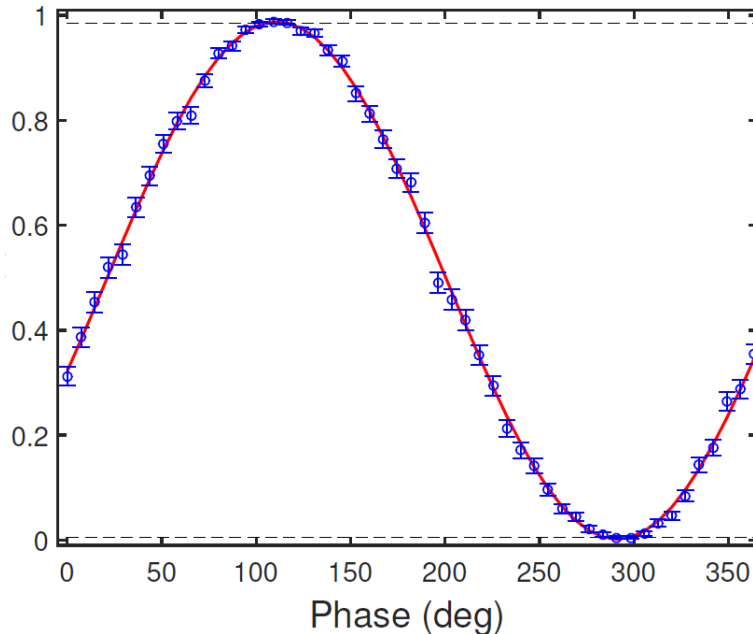
GHZ fidelity > 90%
(technical errors dominate)

Entangled state diagnosis

One ion interference experiment

$$\frac{1}{\sqrt{2}} (|0\rangle + ie^{i\phi} |1\rangle)$$

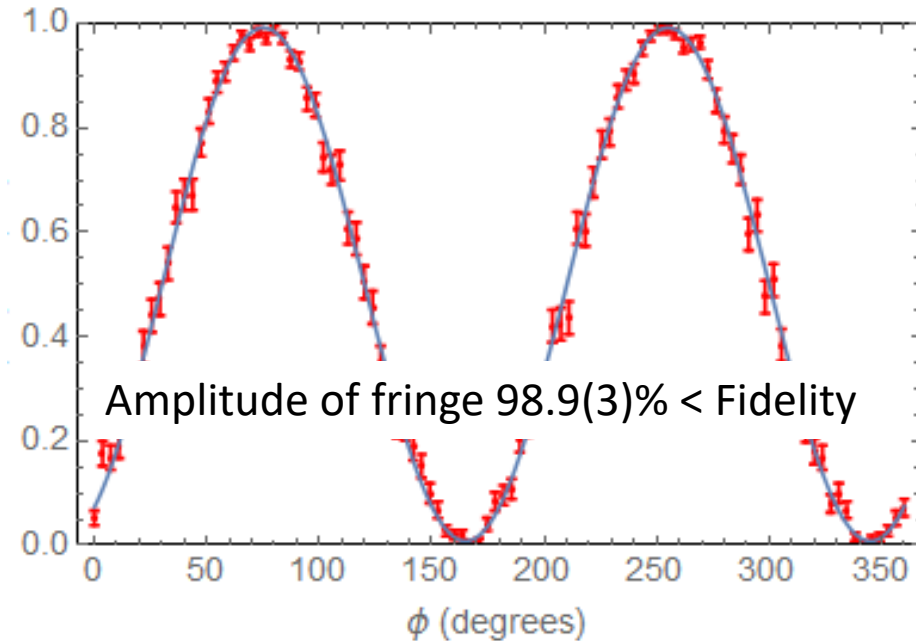
$$P(+\phi_{\pi/2}) = (1 + \cos(\phi - \phi_{\pi/2})) / 2$$



Entangled ions interference experiment

$$|\psi_+\rangle = \frac{1}{\sqrt{2}} (|00\rangle + ie^{2i\phi} |11\rangle)$$

$$P(11) + P(00) = (1 - \cos(2(\phi - \phi_{\pi/2}))) / 2$$

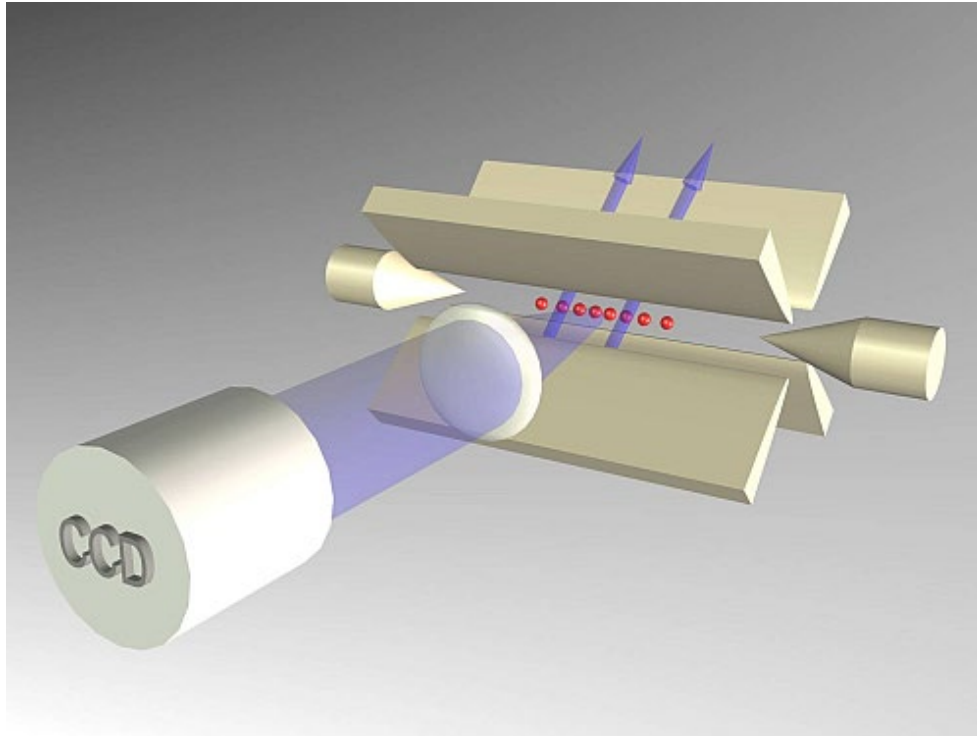


Best results worldwide:

Bell state F = 99.9% (Oxford, NIST, hyperfine)

Bell state F = 99.8% (Innsbruck, optical)

“Linear chain” Trapped-Ion Quantum Computing



Arbitrary single qubit gates

$$U(\theta) = e^{i\theta\sigma_{\alpha}^{(i)}}$$

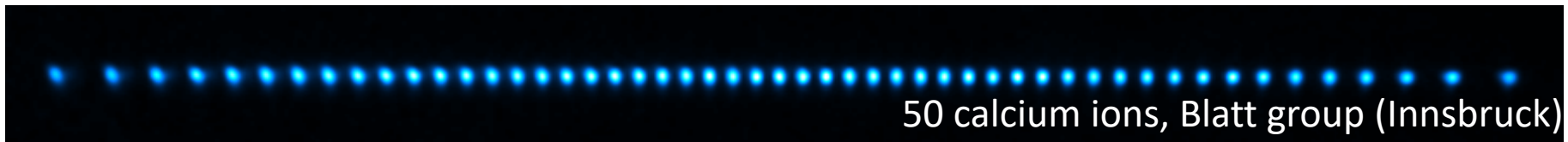
$$\sigma_{\alpha}^{(i)} = \sigma_X^{(i)}, \sigma_Y^{(i)}, \sigma_Z^{(i)}$$

Multi-qubit gates

$$U_{\text{MS}}(\theta) = e^{i\theta S_X^2}$$

$$S_X = \sum_i^{N'} \sigma_X^{(i)}$$

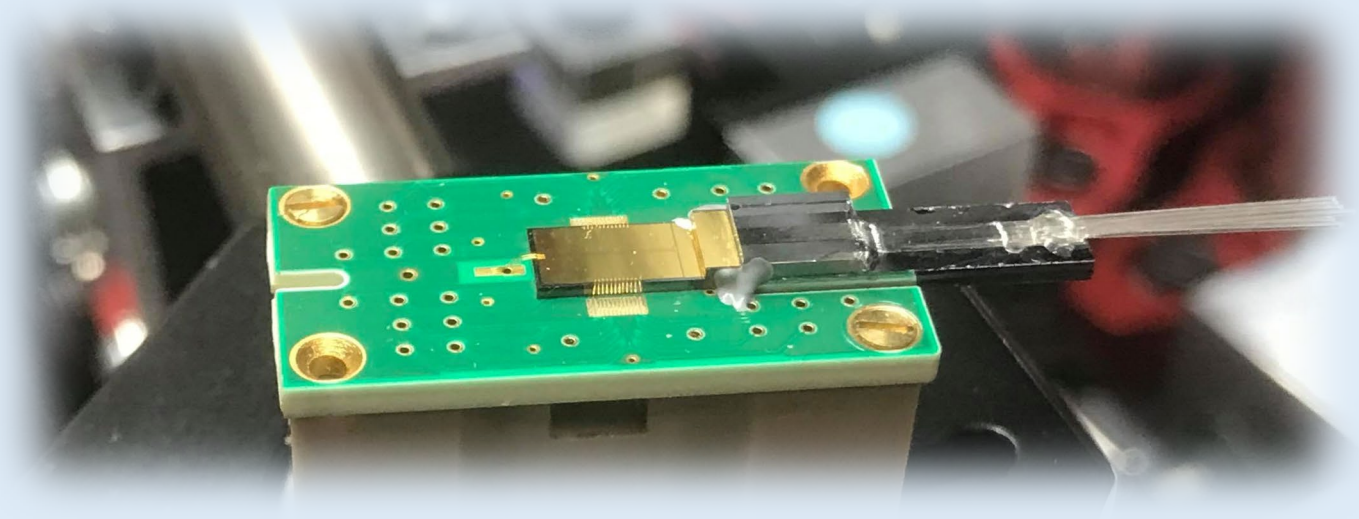
Ion chain is rigid – all ions can be coupled



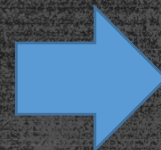
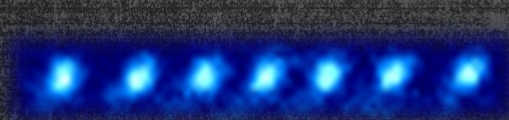
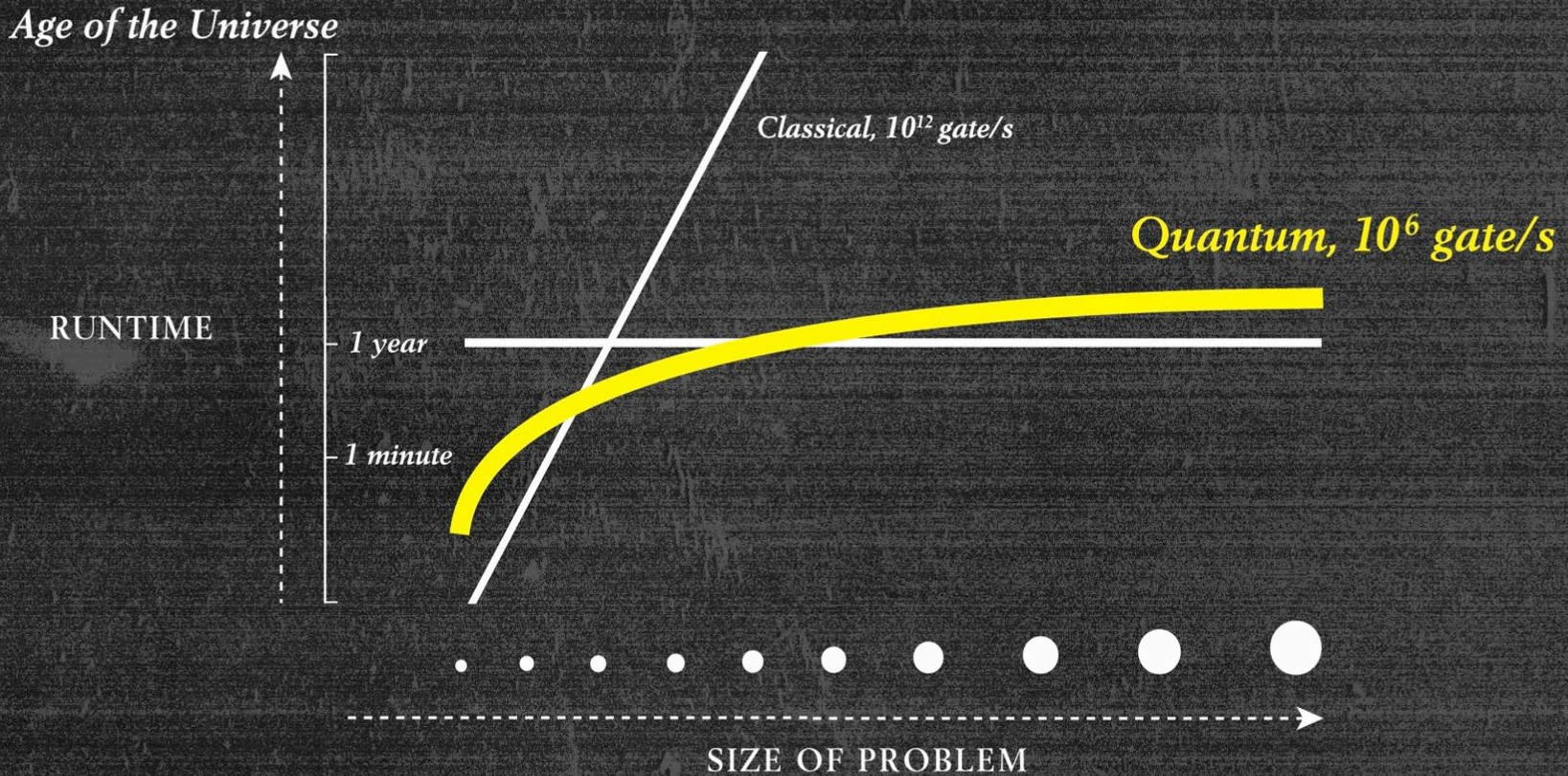
50 calcium ions, Blatt group (Innsbruck)

Most “scalable” approach for near-term NISQ: Monroe + IonQ, Blatt + AQT, etc.

Approaches to scaling



Quantum computers



1 million qubits
 10^{17} gates

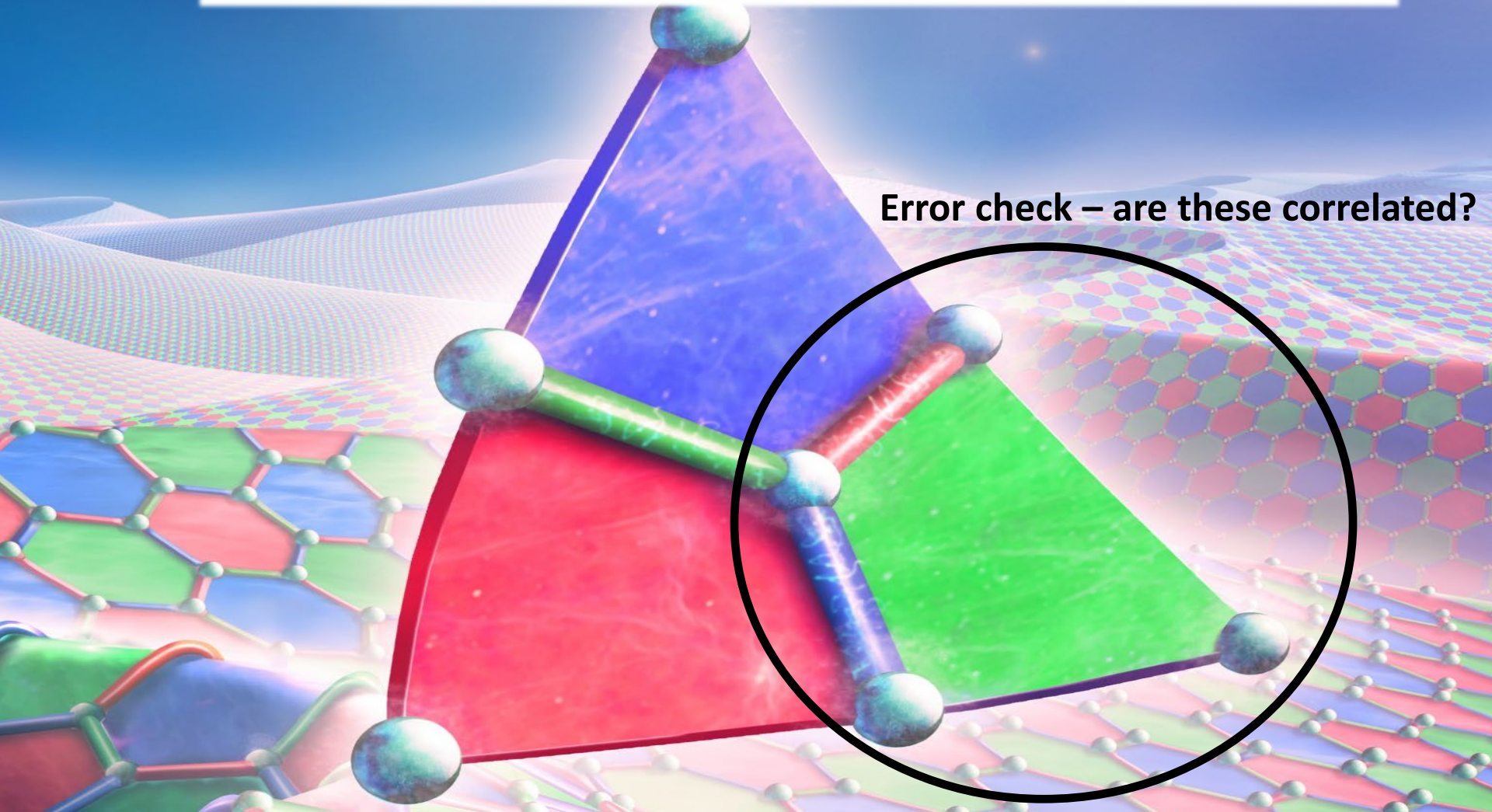
Quantum error correction

Main observation: errors (physics) are mostly local

Solution:

- 1. delocalize information (many qubits required)**
- 2. repeatedly check for errors + correct (good operations)**

Error check – are these correlated?



Scaling path for ion trap QIP

< 100 ions

Extended ion chains



Gate fidelity/speed
limits
applications

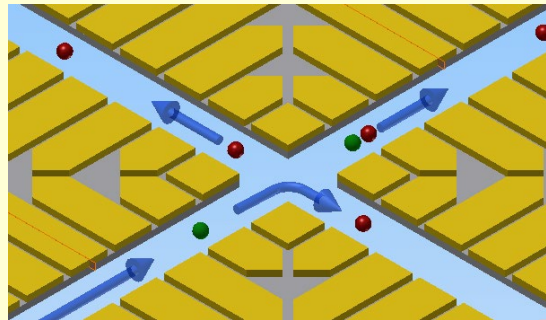
Error-correction?

Intrinsically non-local,
hard to be Fault Tolerant

100-200 ions

Quantum CCD

- Shuttle ions and isolate small numbers
- Parallel zone operation

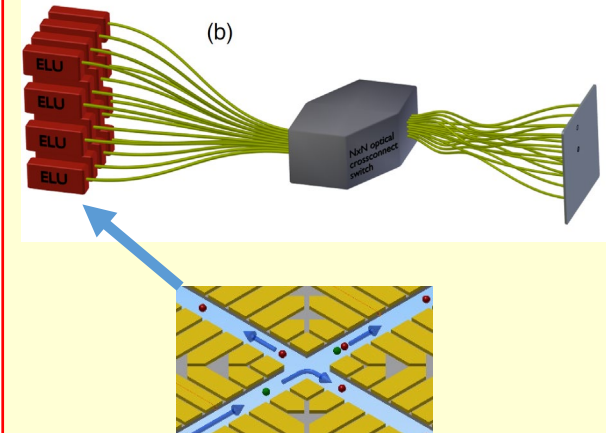


Challenges:

Multi-channels of...
optical integration/delivery
Electrical wiring/fabrication

> 200 ions

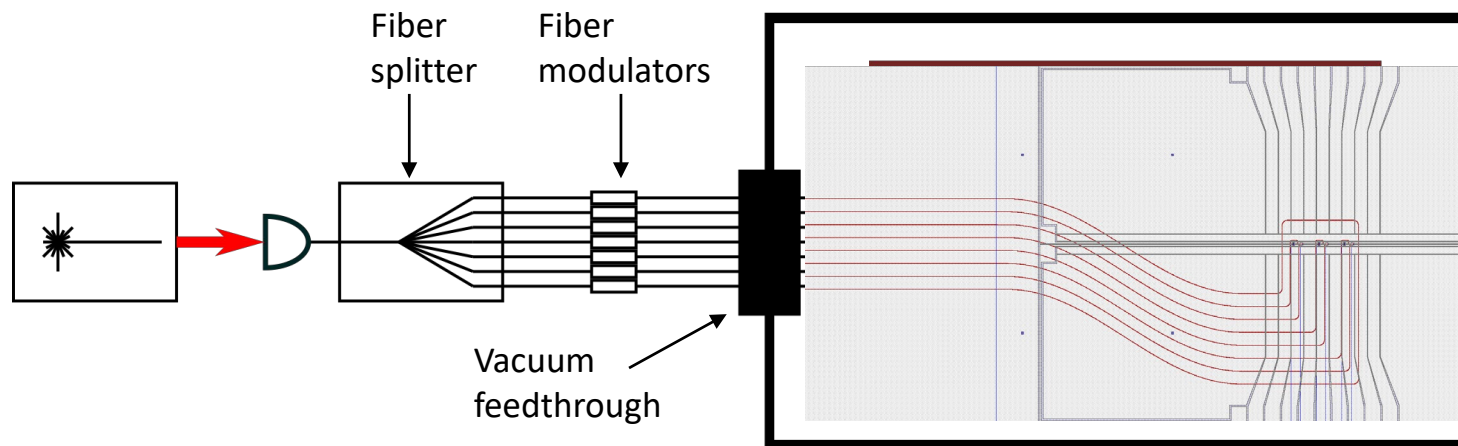
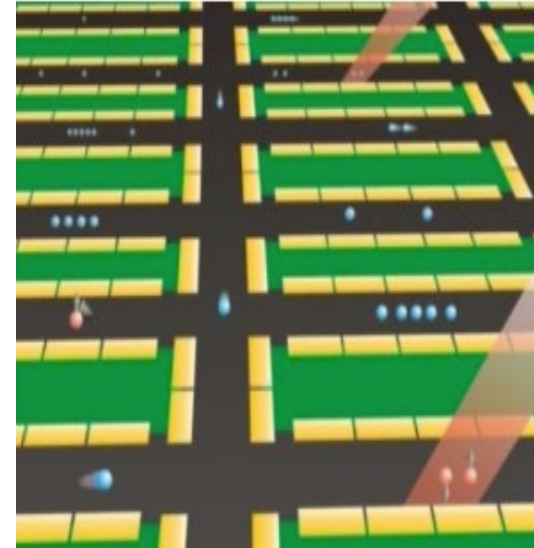
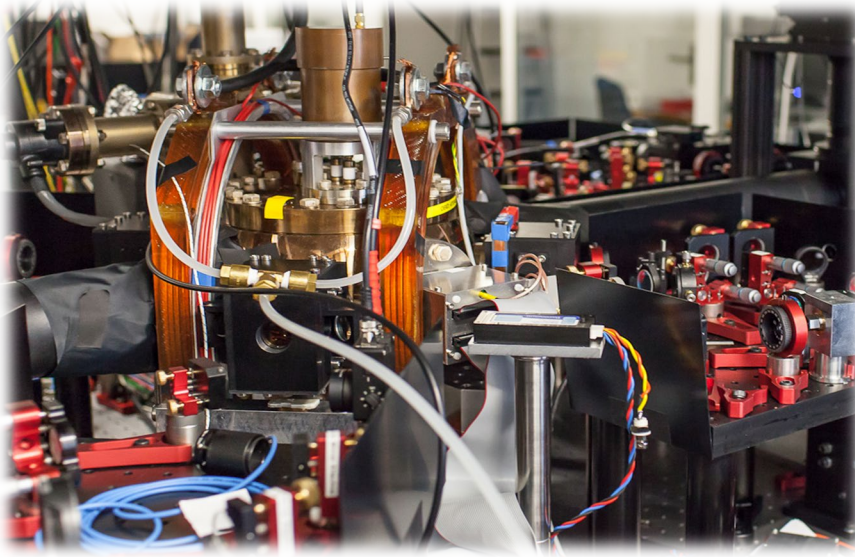
Photonic links



Rate:

How to integrate optical
cavities

Optical wiring of the quantum computer



- MIT + Lincoln labs: K. Mehta *et al.* Nature Nano 11 1066 (2016), Challenge: 33 dB loss from input to ion
- R. J. Niffenegger *et al.*, arXiv 2001.05052 (2020): Delivery near UV and visible light to ions

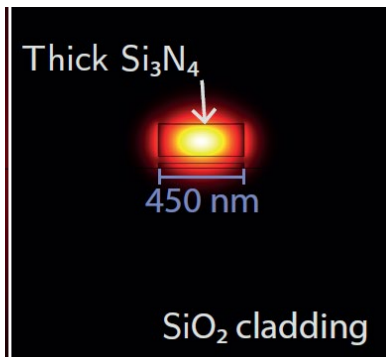
Trap-integrated waveguides

K. Mehta et al. arXiv:2002.03358 (2020)

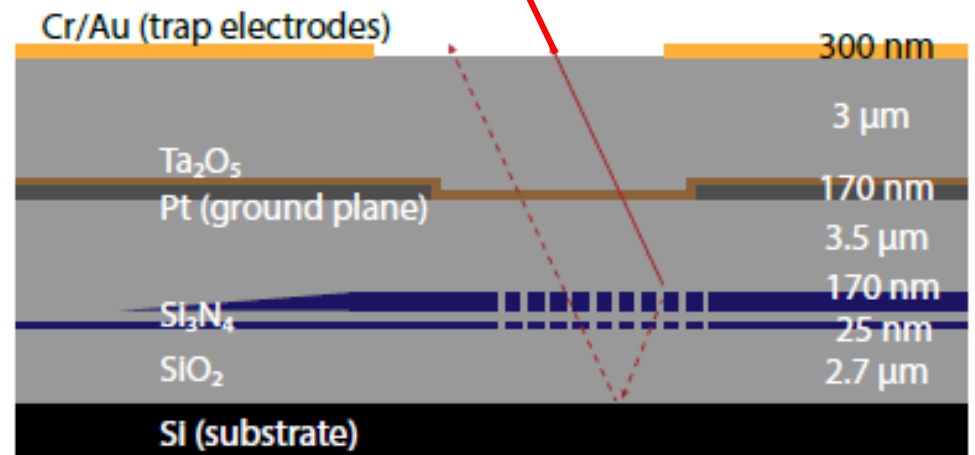
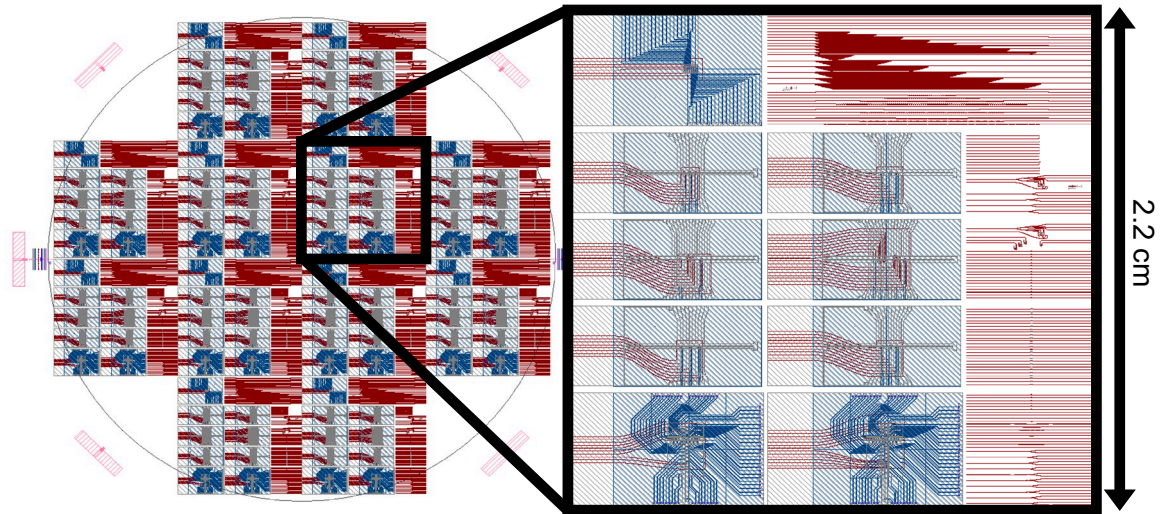
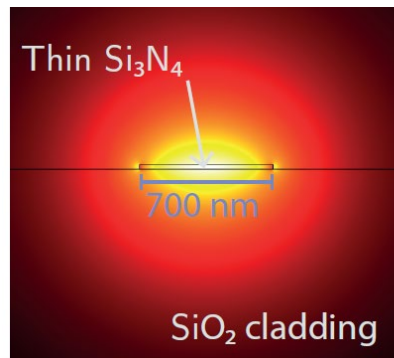
Commercial foundry



Routing

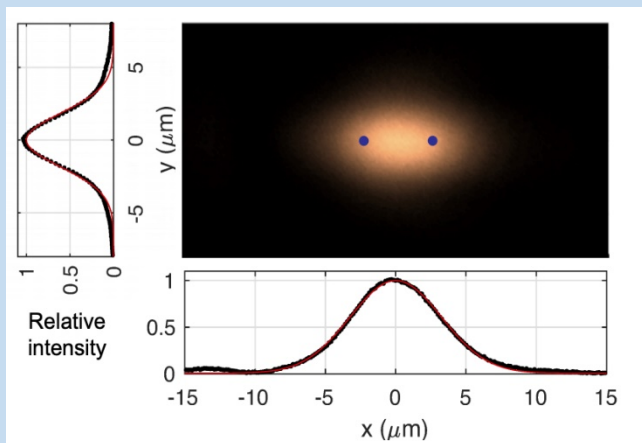


Fiber matching

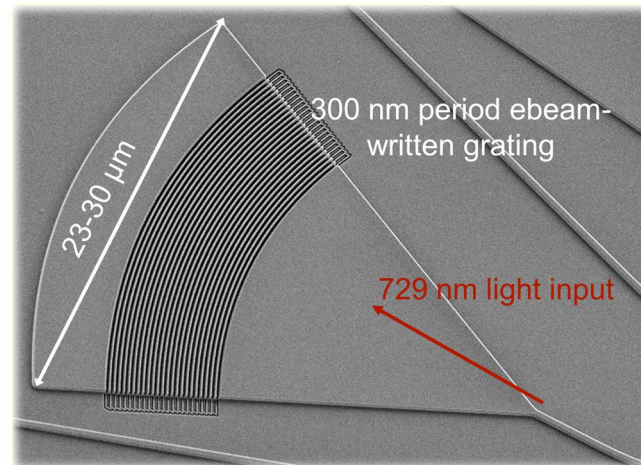


Diffraction to the ion

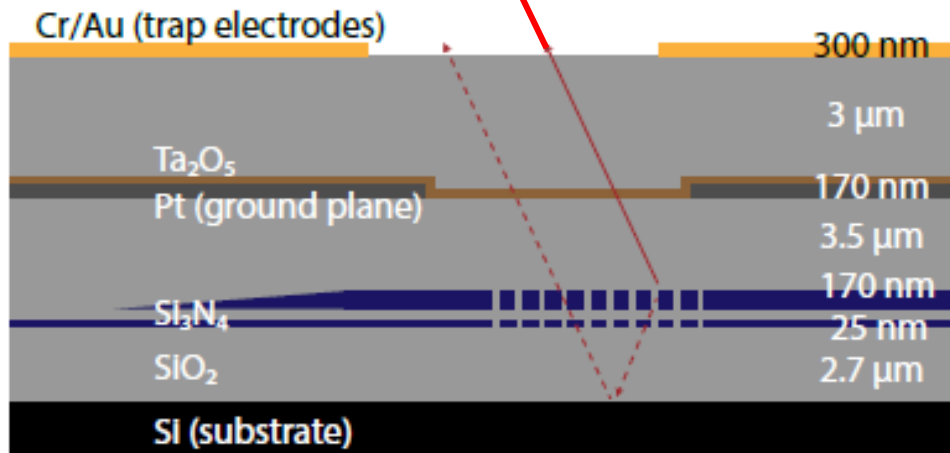
6.5 μm x 3.7 μm focus (2 ions)



Light to ion
50 micron above surface



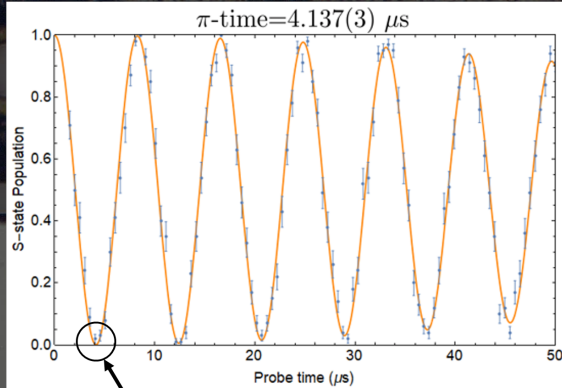
Light input



Integrated waveguide chips: ETH no. 6

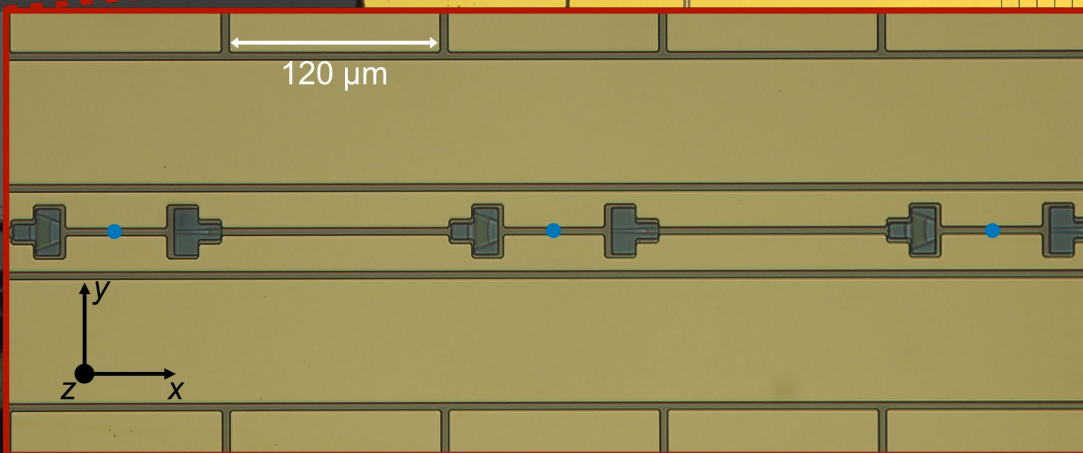
K. Mehta, M. Malinowski, C. Zhang et al. arXiv:2002.03358 (2020)

Using waveguide-delivered light:



4.1 μ s

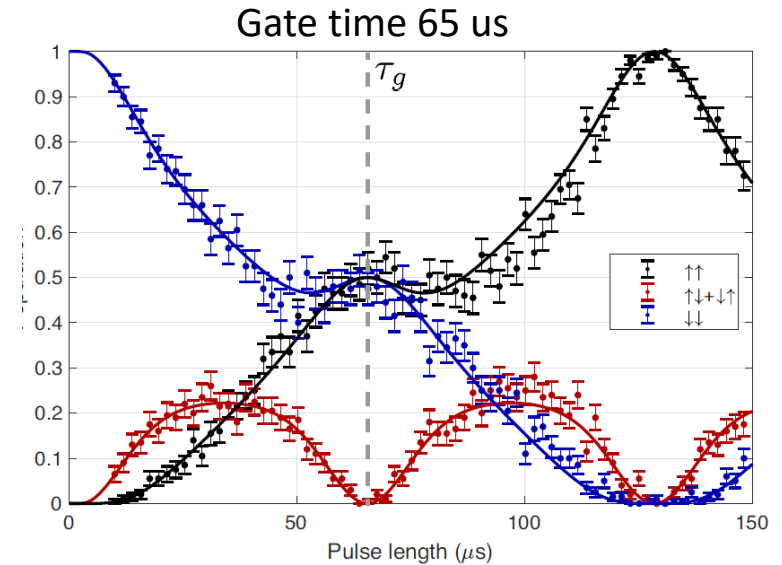
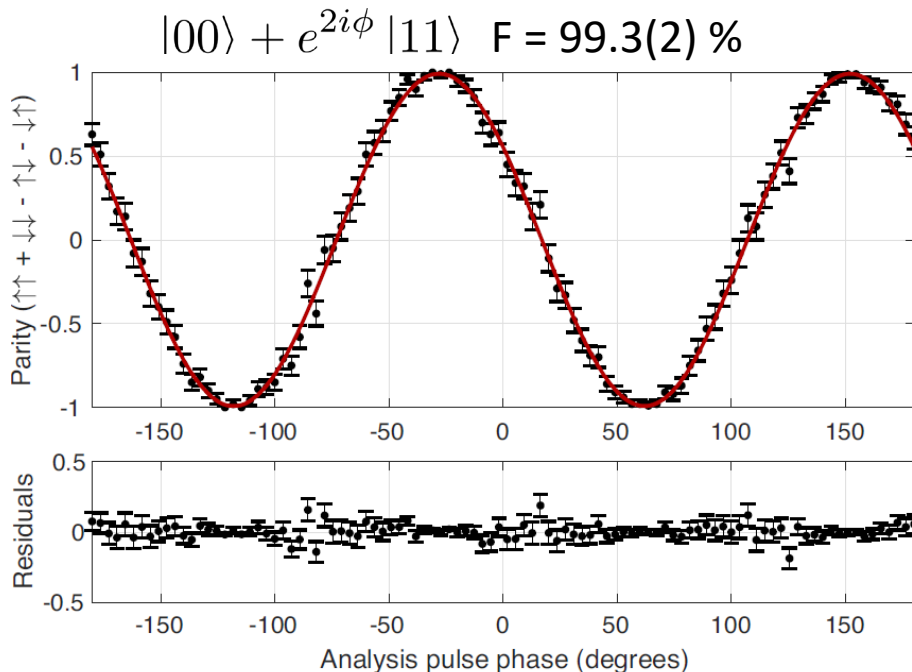
Special attention paid to reducing
Fibre-attach losses to 1.5 dB level at 300 K and 7K



ETH chip 7: Multi-qubit gates using integrated photonics

K. Mehta, M. Malinowski, C. Zhang et al. arXiv:200203358 (2020) Nature, in press

1.5 mW emitted from coupler

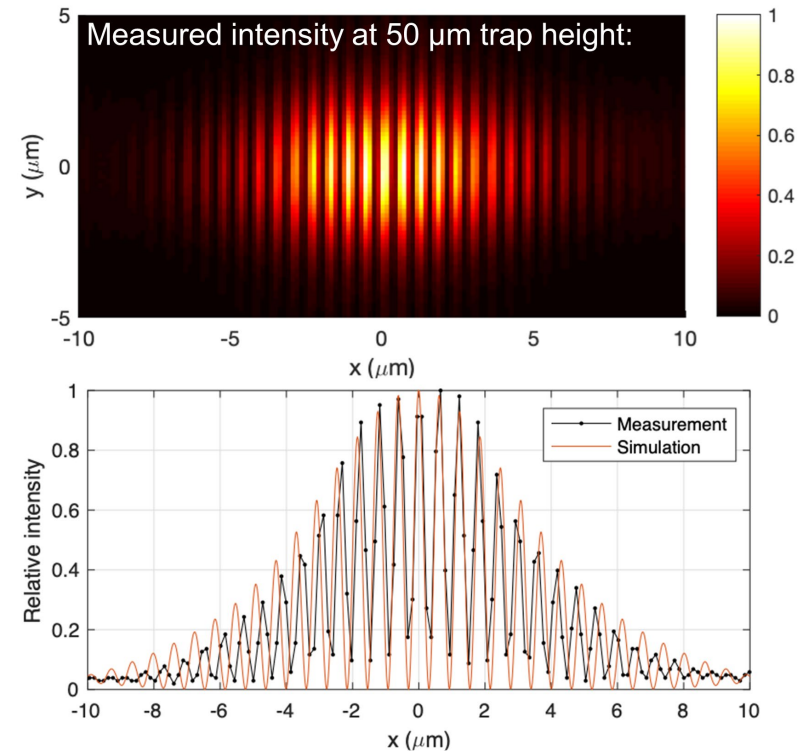
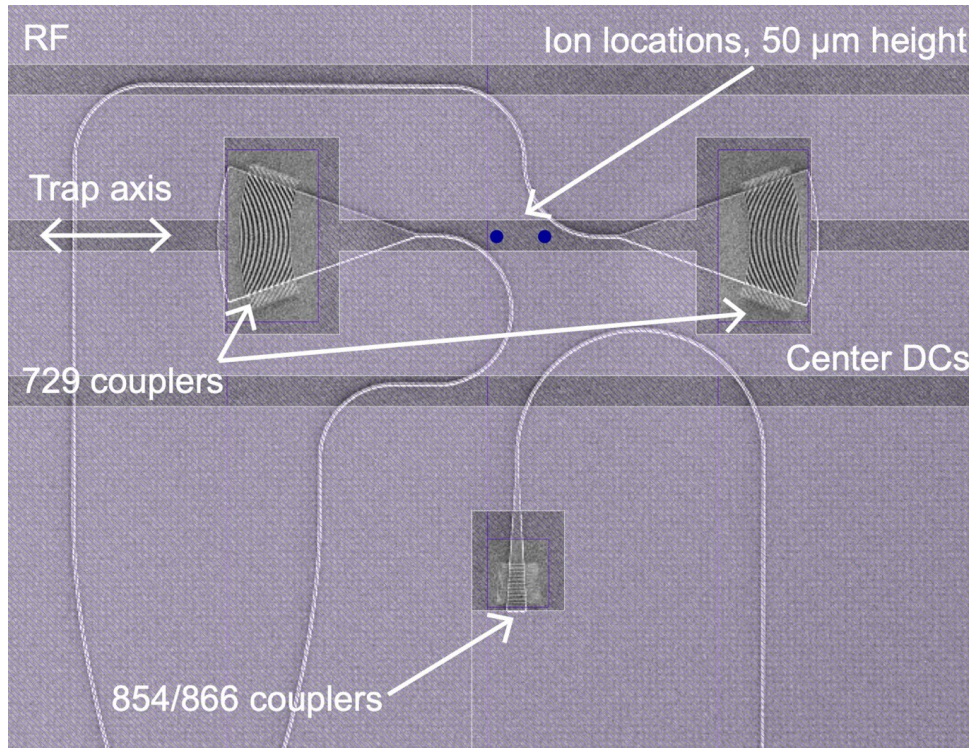


Error source	Infidelity ($\times 10^{-3}$)
Motional mode heating	2(1)
Motional frequency drifts	1
Laser frequency noise	1
Two-ion readout error	0.5
Kerr cross-coupling	0.4
Spectator mode occupancies	0.3
Spontaneous emission	0.03
Total	$\sim 5 \times 10^{-3}$

“Raw” fidelity – mitigation techniques known

Trap-integrated waveguides: standing-wave MS gates

K. Mehta et al. SPIE OPTO (2019)



At anti-nodes we have **gradients** but no field, and vice-versa

Travelling wave “standard” gate

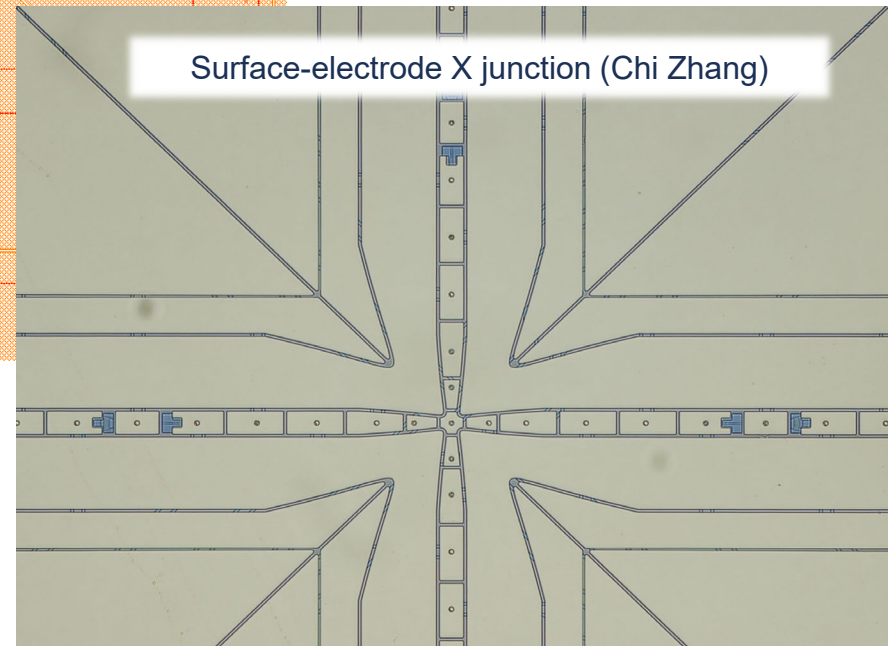
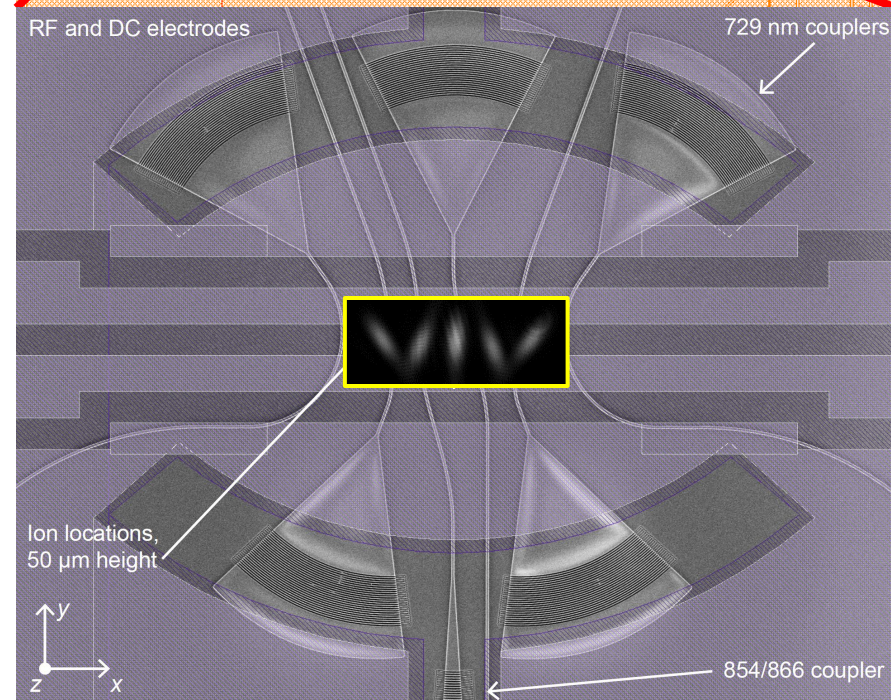
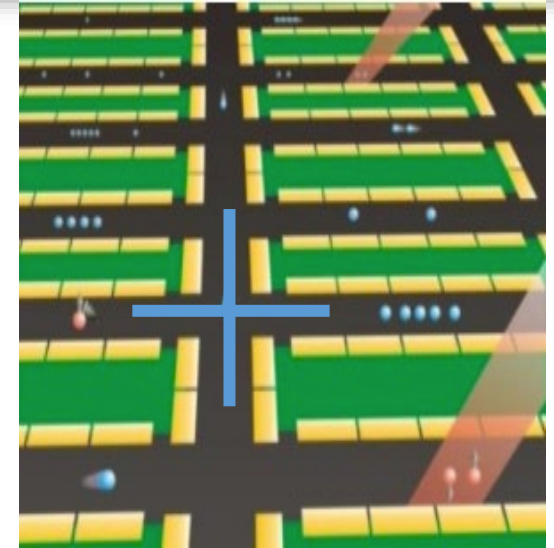
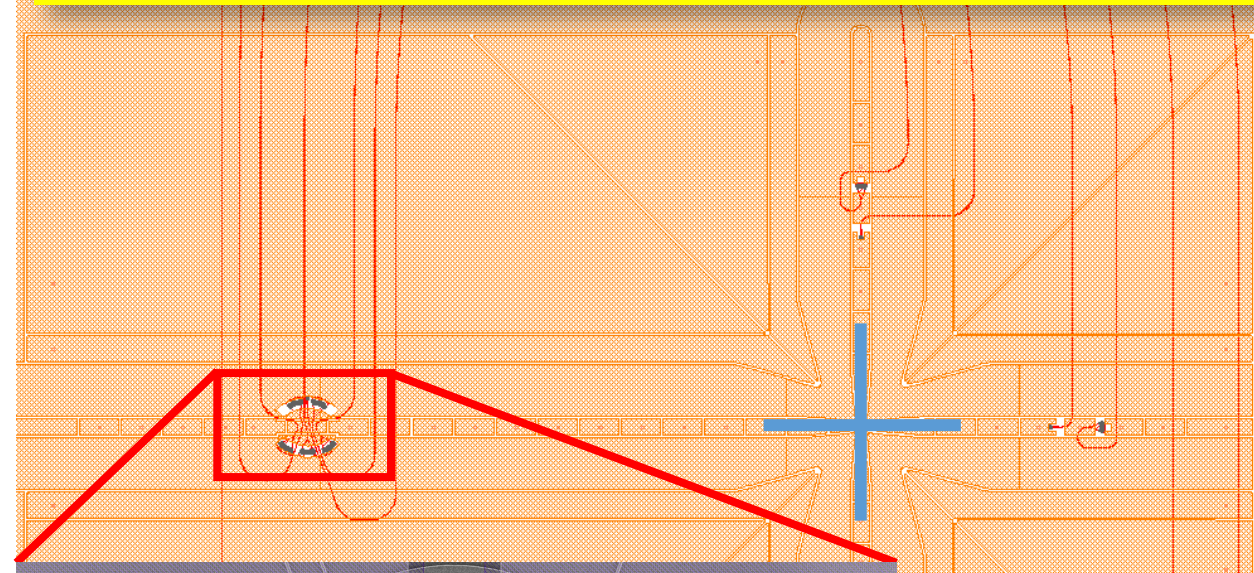
$$E \propto E_0 \sin(kx - \omega t)$$

Standing wave – no direct spin drive at node

$$E \propto E_0 \sin(kx) \sin(\omega t)$$

Enables MS gate without limitation of off-resonant carrier drive

Trap-integrated waveguides: beyond a single zone



Scaling up – challenges of RF traps

Radio-frequency trap

$$V_{\text{static}}(\mathbf{r}) + \Phi_{\text{RF}}(\mathbf{r})$$

- RF null intrinsically 1-D
- Co-alignment of RF and static potentials
- Heating of ion trap chips

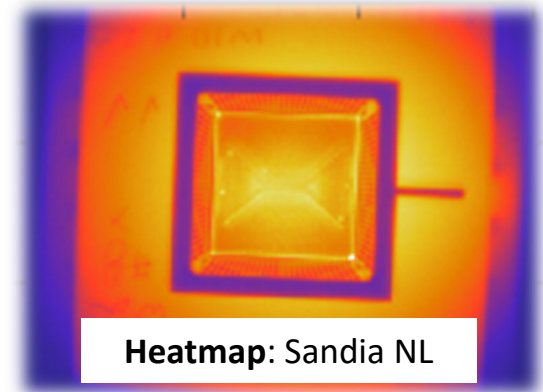
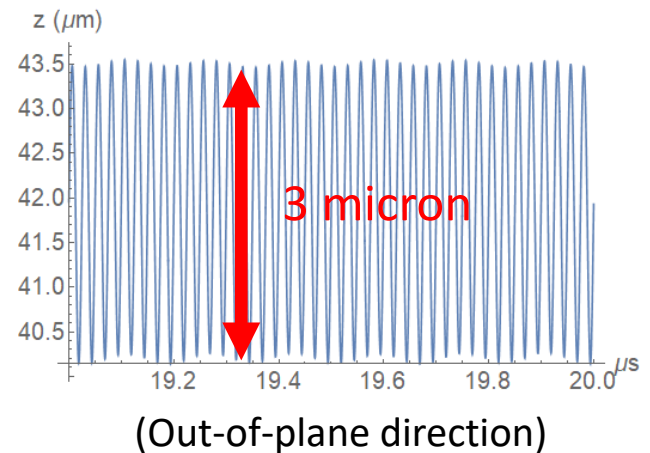
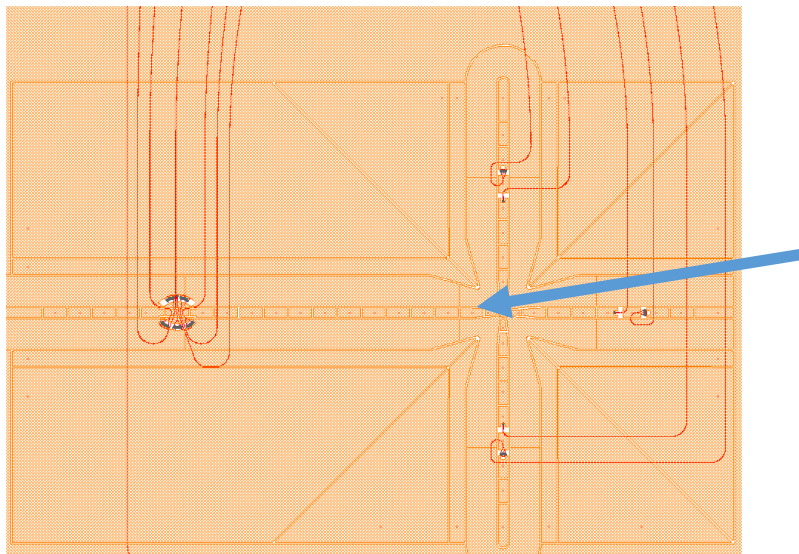


Image: T. Monz, R. Blatt, U. Innsbruck



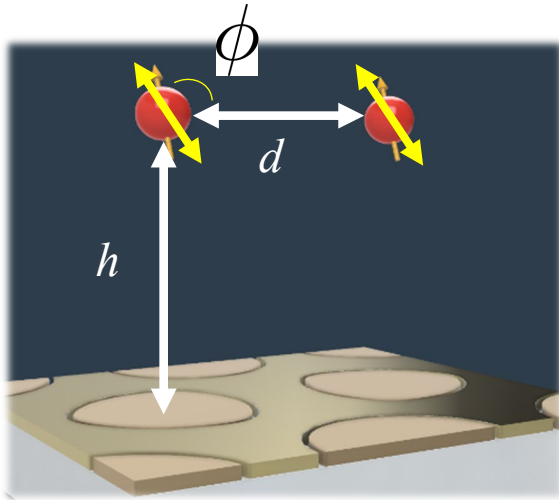
Junction trap
with waveguides
(Chi Zhang)



Individual ions in micro-traps

RF traps @ NIST, Freiburg, Sussex

Closely spaced 0-dimensional static + RF potentials $\sum_i V_i(\mathbf{r}_i) + \sum_i \Phi_{\text{RF},i}(\mathbf{r}_i)$



Normal modes split similar to dipole-dipole coupling

$$\Omega_{\text{ex},z} (1 - 3 \cos^2(\phi)) (a_i a_j^\dagger + a_j a_i^\dagger)$$

$$\Omega_{\text{ex},z} = \frac{e^2}{4\pi\epsilon_0 M \omega_z d^3} \propto \frac{z_0^2}{d^3} \quad \leftarrow \text{Zero point motion}$$

- Hard to get small scales – anomalous heating limits height
- Limited mode splitting limits spectral isolation for 2-qubit gates

2-qubit gate: Wilson et al. Nature 512, 57–60(2014)

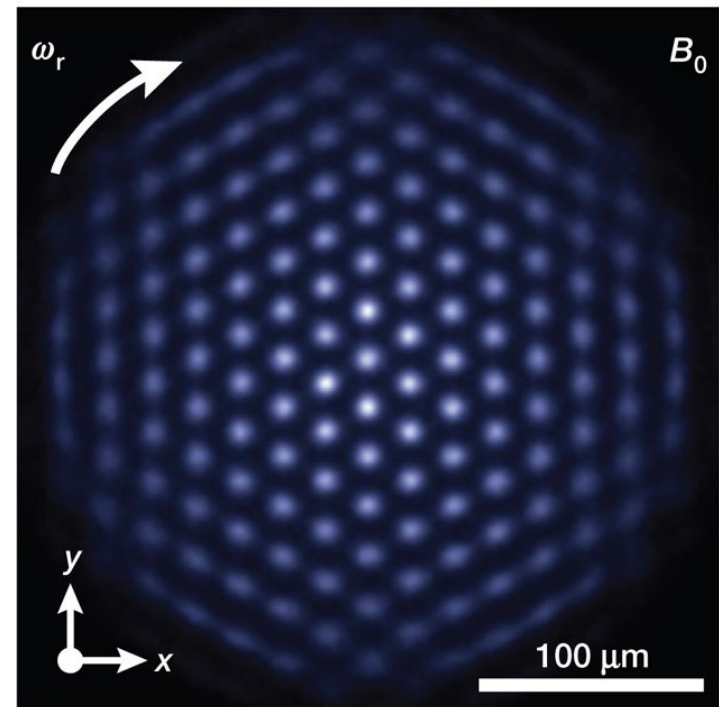
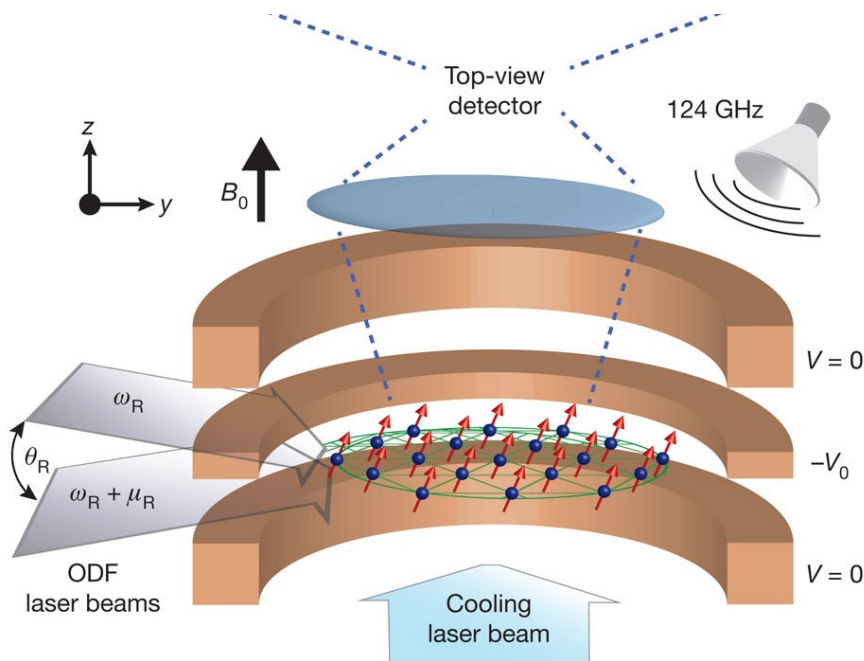
Penning traps

Multi-ion crystals + quantum control: NIST, Imperial, Sydney

$$V(z^2 - (x^2 + y^2)/2) + \{\mathbf{B}\hat{z}\}$$

Single potential well – (rotating) ion crystals of > 100 ions

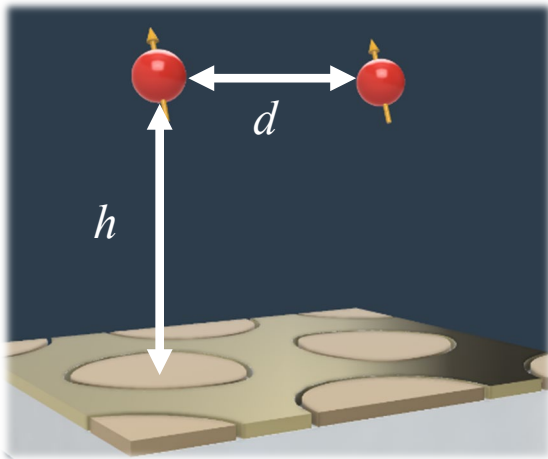
J. Bollinger et al, NIST



Penning trap arrays

S. Jain, J. Alonso, M. Grau et al. PRX, 10, 3, 031027 (2020)

$$\sum V_i(\mathbf{r}_i) + \Phi_{\text{RF},i}(\mathbf{r}_i) \quad \longrightarrow \quad \sum_i V_i(\mathbf{r}_i) + \{\mathbf{B}\}$$



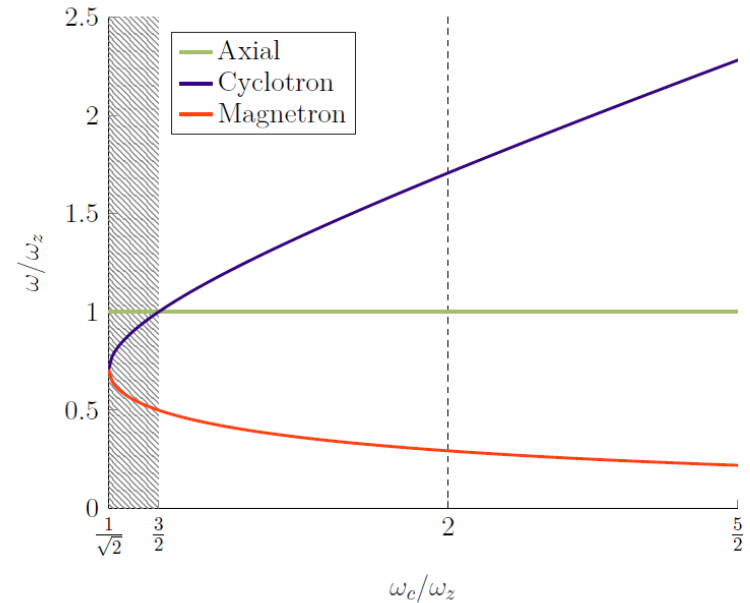
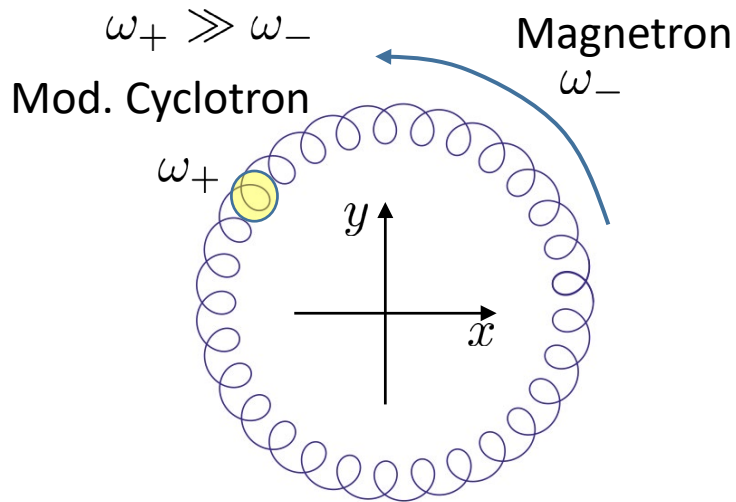
Static potentials stronger than RF pseudopotentials
Lower voltage for same trap spacing

$$\| \Psi_{\text{RF}}^{(2)} \| = \underbrace{\frac{\sqrt{3}}{8} |q_z|}_{\text{P.P. curvature}} \cdot \| \Pi^{(2)} \| \quad \text{Static curvature}$$

$\sim 1/16$

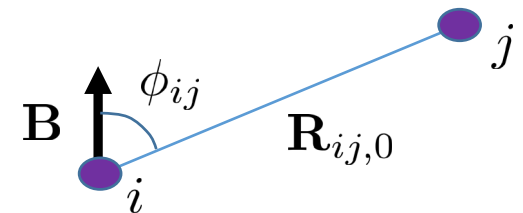
- Traps use only static fields
- Reduced sensitivity to stray fields (B field is homogeneous)
- Power dissipation minimal (during cooling)

Couplings + zero-point motion



Neighboring similar traps: Coulomb couplings (perturbative)

$$(-1)^\nu \Omega_{\text{ex},\nu} (1 - 3 \cos^2(\phi_{ij})) (a_i a_j^\dagger + a_j a_i^\dagger)$$



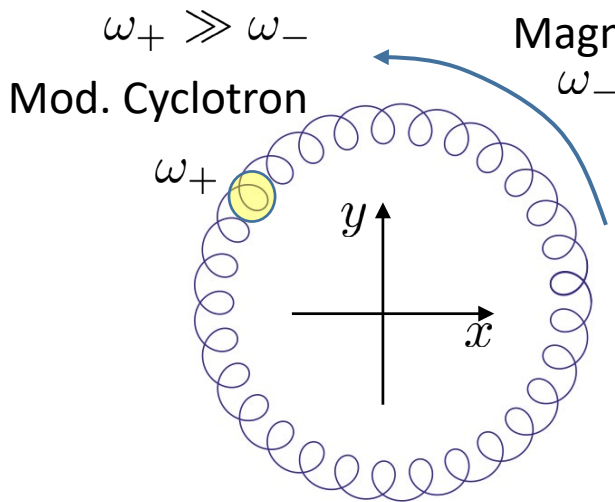
Dipoles **for all modes** act as if they point along the B field

$$\Omega_{\text{ex},z} = \frac{e^2}{4\pi\epsilon_0 M \omega_z d^3}$$

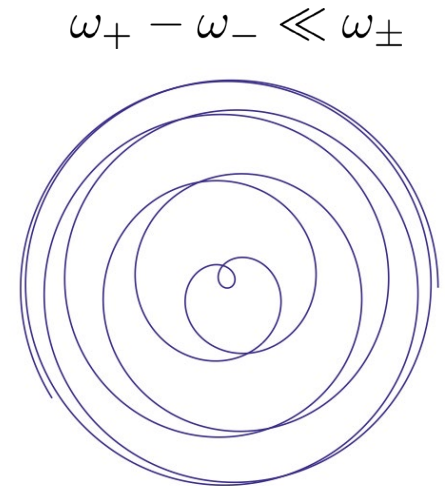
$$\Omega_{\text{ex},\pm} = \frac{e^2}{4\pi\epsilon_0 M (\omega_+ - \omega_-) d^3}$$

Enhanced zero-point motion: consequences

Zero-point motion relates to frequency at which potential energy is modulated



$$z_0 = \sqrt{\frac{\hbar}{2m(\omega_+ - \omega_-)}}$$



- couplings enhanced

$$\Omega_{\text{ex}} \propto z_0^2$$

- Laser or B-field
motion coupling enhanced

$$\Omega_g \propto kz_0\Omega \text{ or } \Omega \propto z_0\partial_z B$$

- Heating “enhanced”

$$\dot{\bar{n}}_+ = \frac{e^2}{4m(\omega_+ - \omega_-)} S_E(\omega_+)$$

Enhancement \rightarrow

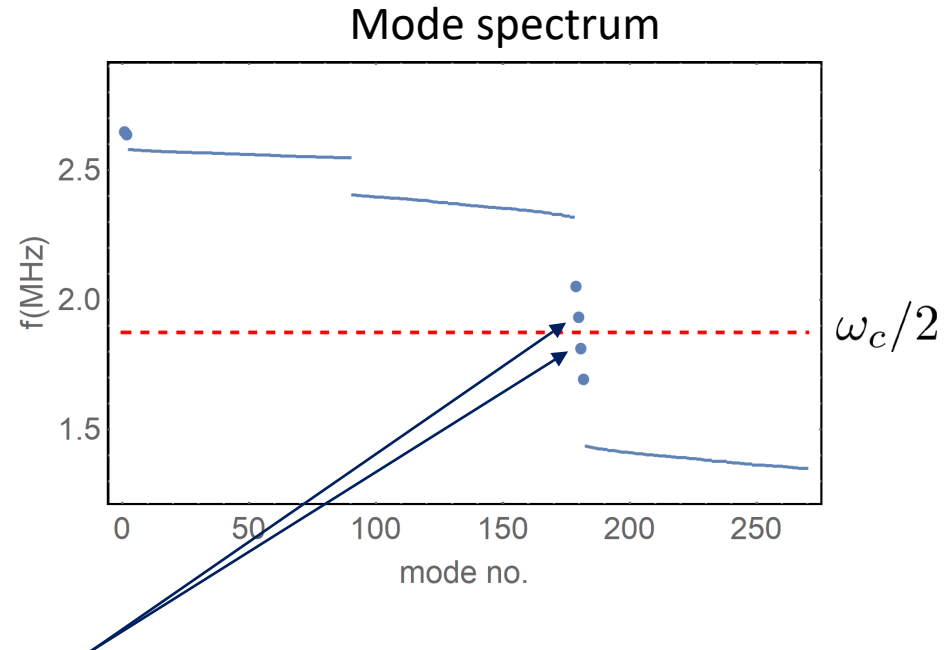
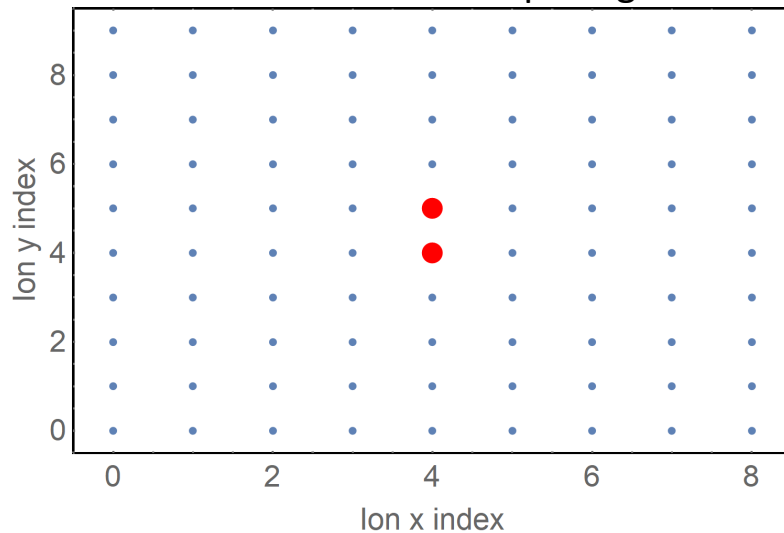
\leftarrow Noise sampling frequency

Quantum computation on a fixed lattice

S. Jain, J. Alonso, M. Grau et al. PRX, 10, 3, 031027 (2020)

Selective tuning of ion frequencies to “large” zero-point motion

Example: 90 beryllium ions, B-field in-plane,
30 micron ion spacing



“Stretch” modes: $\delta/(2\pi) \simeq \pm 60$ kHz, $z_0 \simeq 96$ nm

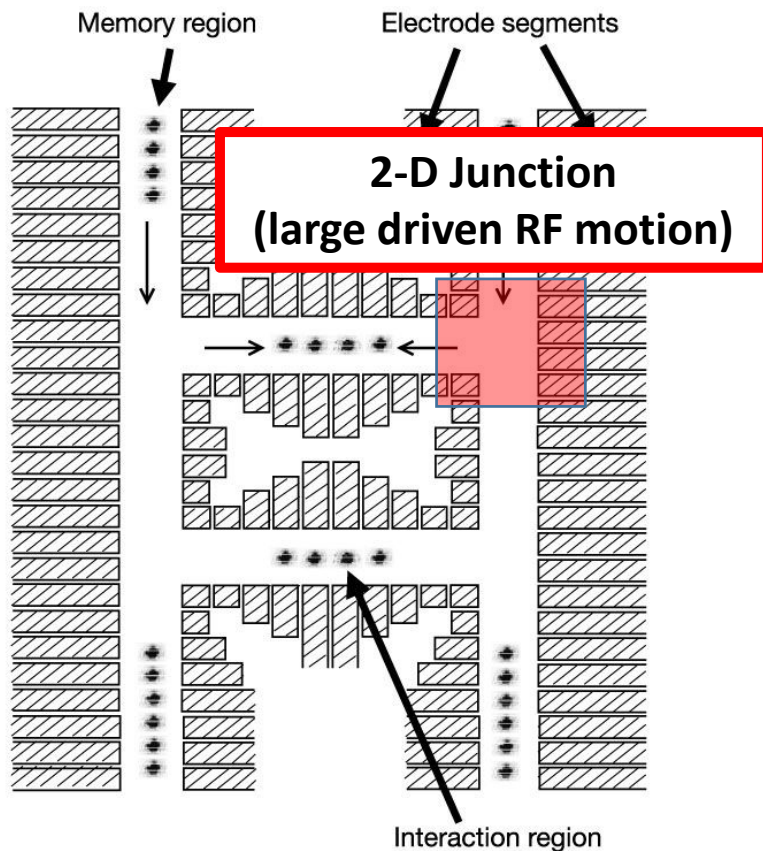
Well isolated + large zero-point motion: good for 2-qubit gate!

Laser “gate” drive at $\mu \simeq \omega_c/2$

“Theoretical” $F > 0.9998$ in 16 microseconds, $\Omega_c = 2\pi \times 300$ kHz, $\Delta\phi = \frac{\pi}{40}$

Quantum computation on a movable lattice

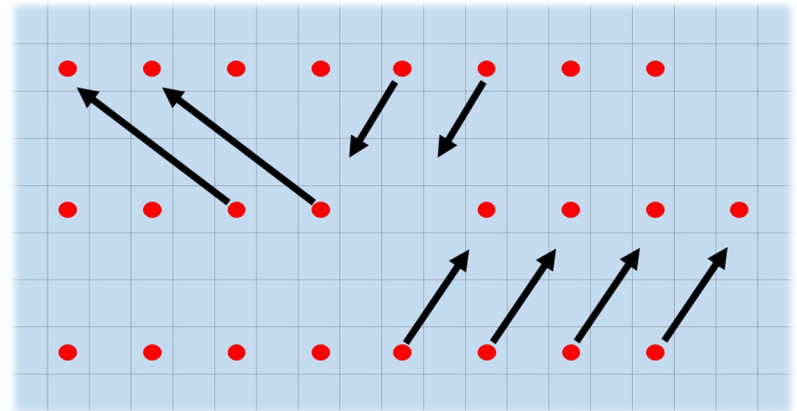
Kielipinski et al. Nature (2002)



Penning: 2-D transport at any position

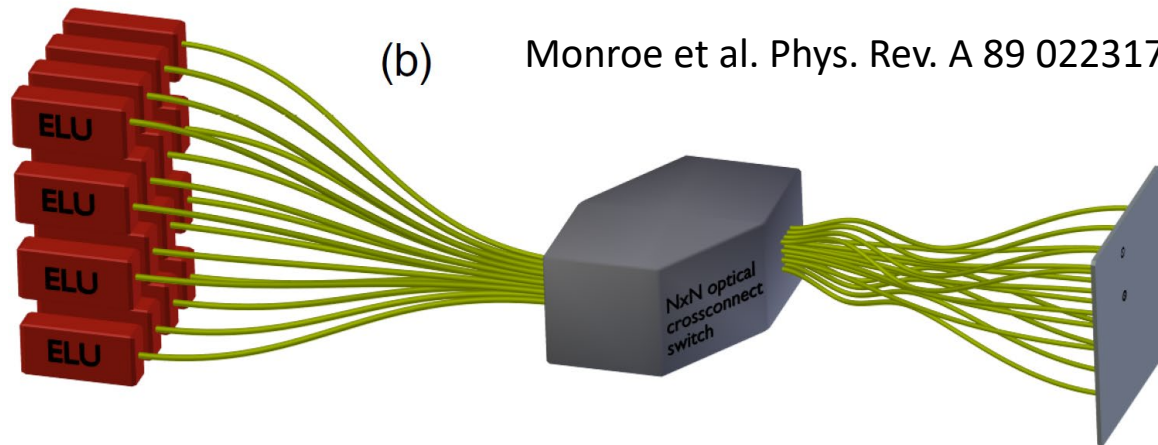
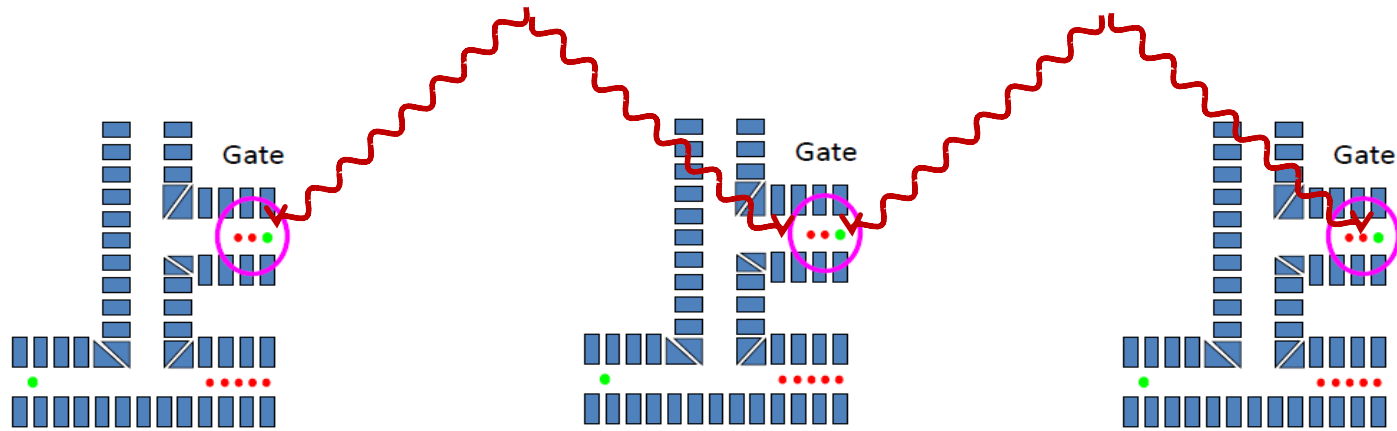
Homogeneous magnetic field

- 3-dimensional transport accessible
 - stray fields primarily cause frequency shifts
- Previous work: Hellwig et al. NJP 12 065019 (2010)
Crick et al. RSI 81, 01311 (2010)

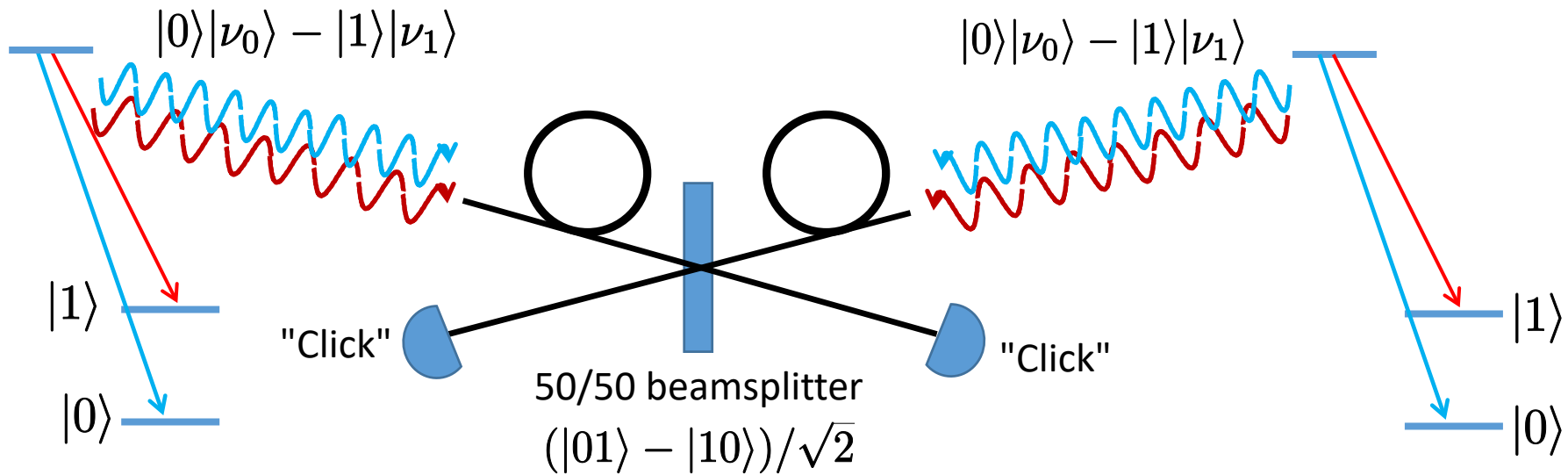


Optical connections

Multiple small processors linked by probabilistic entanglement generation and teleportation



Probabilistic remote entanglement generation

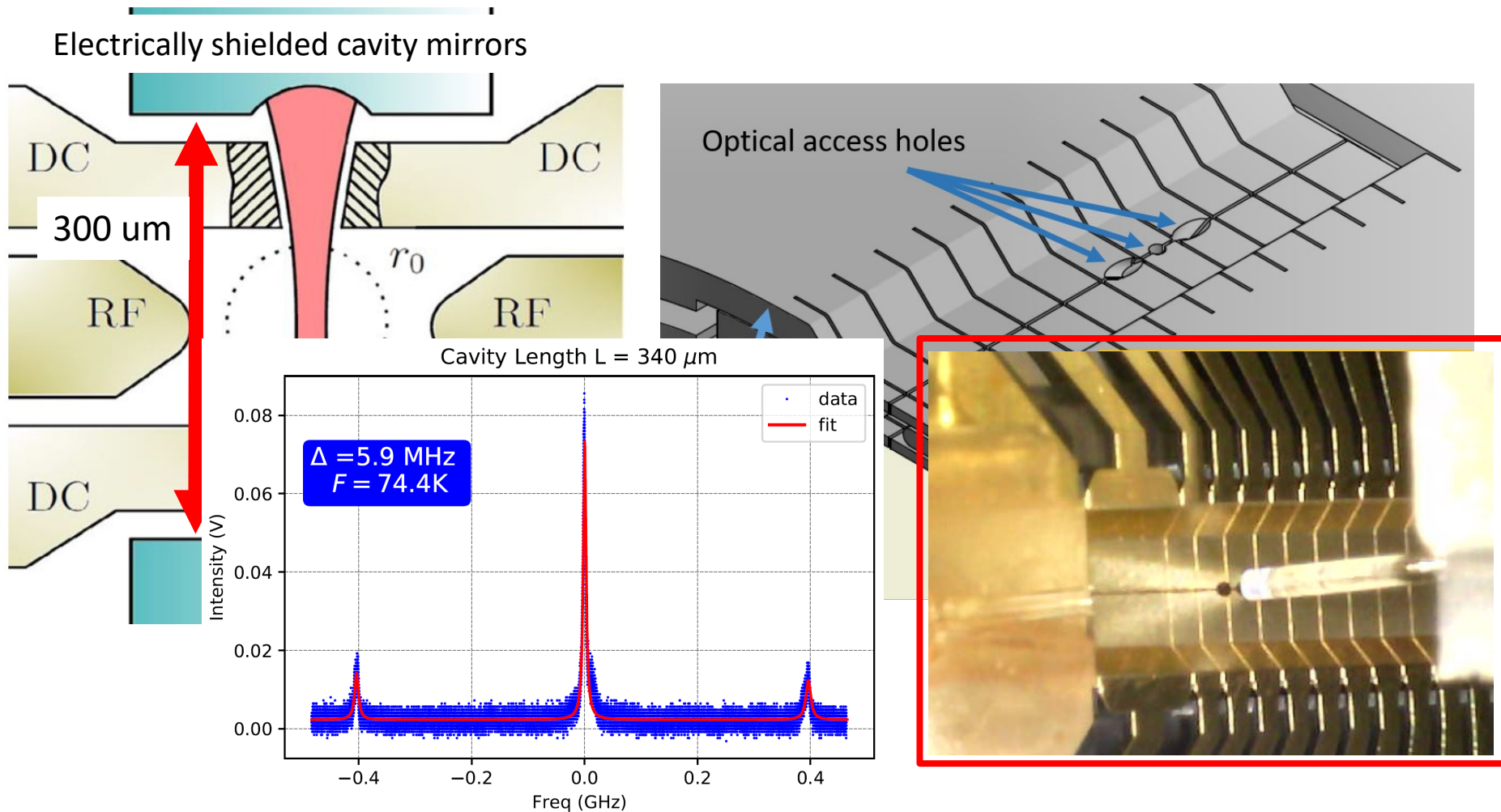


- Entangled ions separated by **1m** (Moehring et al. Nature 449, 68 (2008))
- More recent: entanglement rate up to 180 Hz ((2020))

Ultimately requires optical cavities for higher rates.

Efficient single ion – single photon interfaces

Single-atom \rightarrow single photon: optical Fabry-Perot cavity
Must shield charge of ion from charges on mirror surfaces

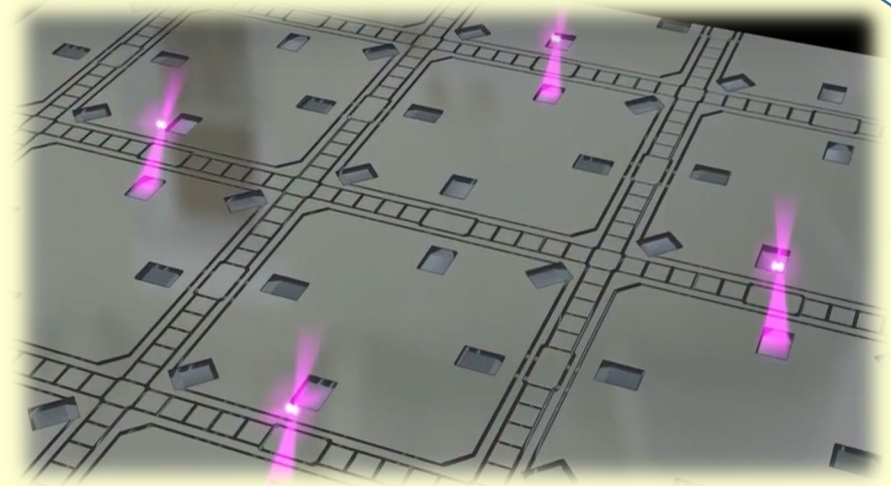


Summary of TIQI results

Integrated optics for quantum control

- High-fidelity multi-qubit gates

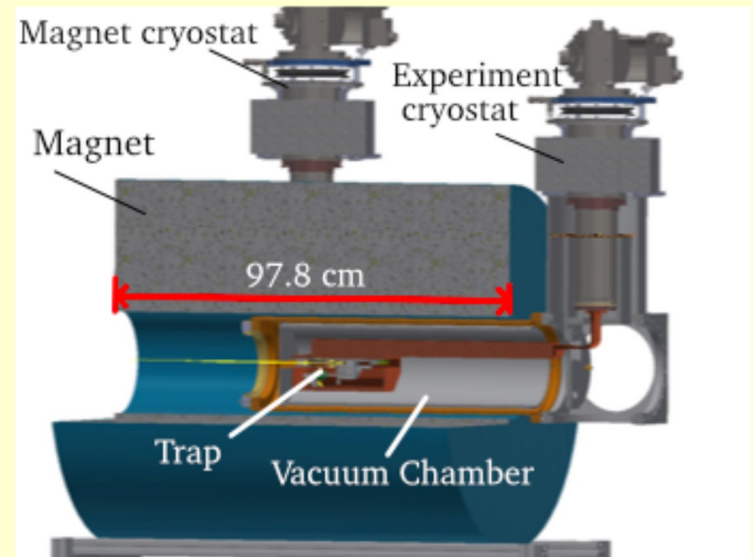
K. Mehta et al. arXiv:200203358 (2020)



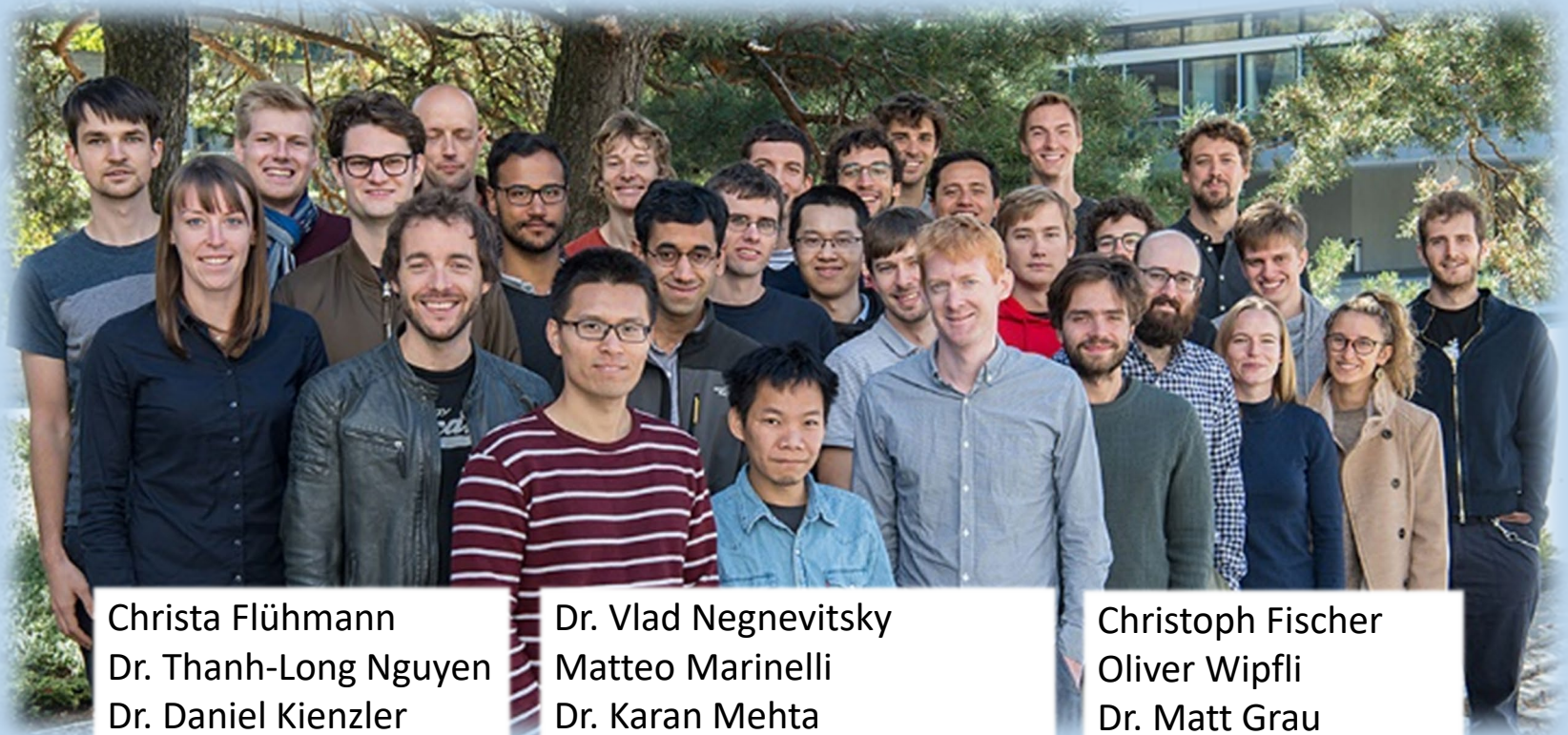
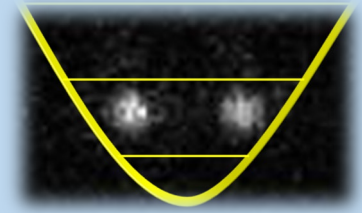
Micro-Penning traps for scaling to 2D

- Quantum simulations
- Quantum computation

S. Jain et al. PRX, 10, 3, 031027 (2020)
(Multi-ion invariance, theory of normal modes)



Trapped Ion Quantum Information Group
ETH Zürich
www.tiqi.ethz.ch



Christa Flühmann
Dr. Thanh-Long Nguyen
Dr. Daniel Kienzler
Robin Oswald
Roland Matt
Chiara Decaroli
Simon Ragg
Dr. Thomas Lutz
Dr. Celeste Carruth

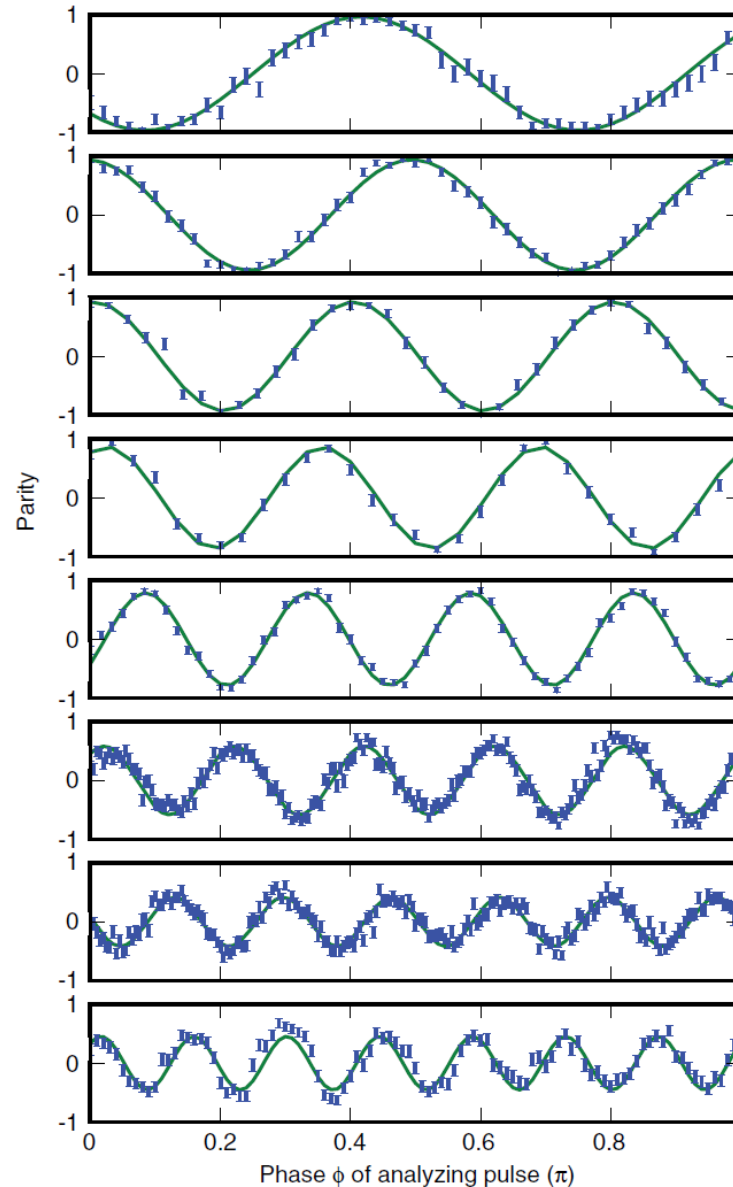
Dr. Vlad Negnevitsky
Matteo Marinelli
Dr. Karan Mehta
Tanja Behrle
Francesco Lancelotti
Brennan McDonald deNeeve
Maciej Malinowski
Chi Zhang

Christoph Fischer
Oliver Wipfli
Dr. Matt Grau
Shreyans Jain
Nick Schwegler
Tobias Saegasser
Dr. Chris Axline
Martin Stadler

GHZ States of up to 14 ions

Monz et al., PRL 106, 130506 (2011), Innsbruck – Blatt group

$$(|11\dots 1\rangle + |00\dots 0\rangle) / \sqrt{2}$$



3 High contrast – 3 ions

4

5

6

8

10

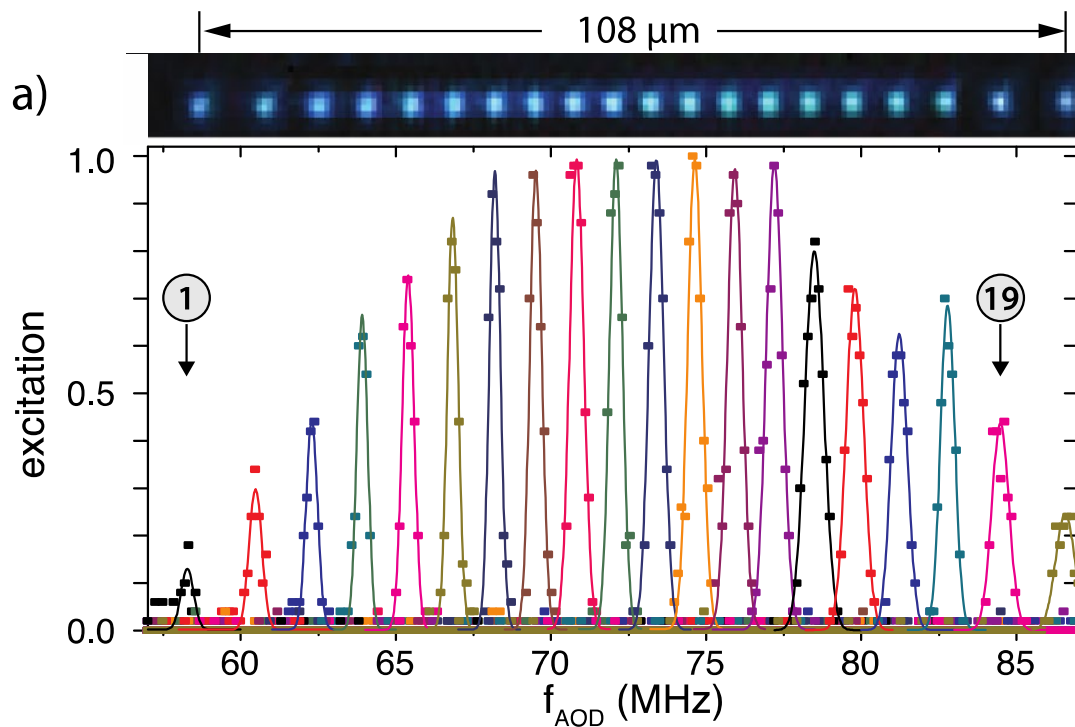
12

14

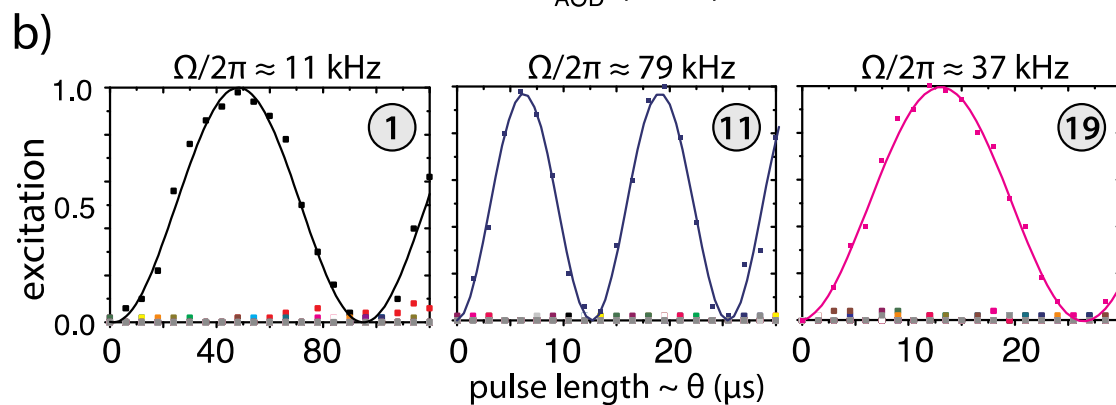
Reduced contrast – 14 ions

Individual rotations on a long ion string

Data: C. Hempel, C. Roos, R. Blatt (Innsbruck)



Global Ramsey,
Individually addressed Stark



Engineered spin-spin interactions

Go to limit of large motional detuning
(very little entanglement between spin and motion)

$$\Omega \ll \delta$$



$$\Phi_{10} = \Phi_{01} \simeq \frac{\Omega^2}{\delta} t$$

$$\frac{1}{2} (|00\rangle + |10\rangle + |01\rangle + |11\rangle)$$

↓ ↓ ↓ ↓

$e^{i\pi/2}$

$$\frac{1}{2} (|00\rangle + i|10\rangle + i|01\rangle + |11\rangle)$$



$$\hat{H}_{\text{eff}} = J \hat{\sigma}_{z,1} \hat{\sigma}_{z,2}$$

Allows creation of many-body Hamiltonians

(Friedenauer et al. Nat. Phys 4, 757-761 (2008))

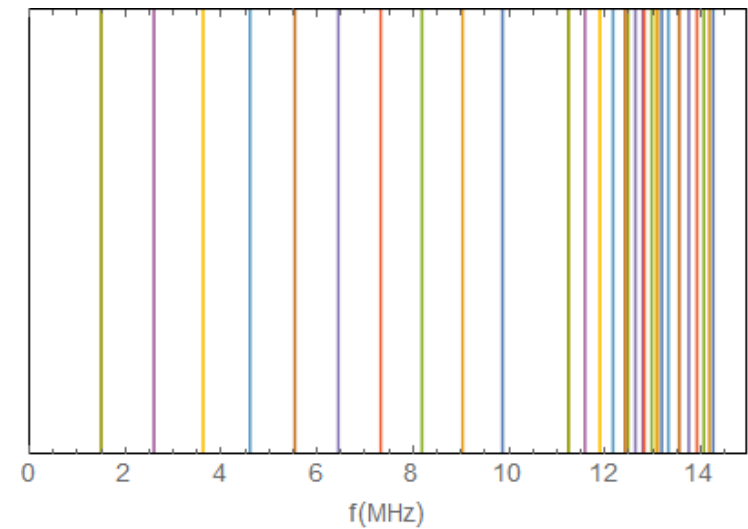
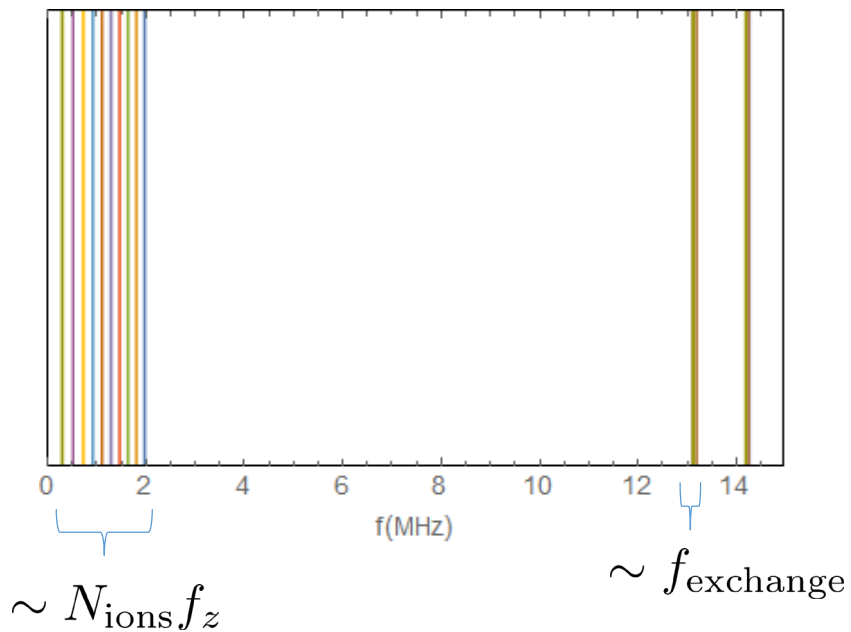
Kim et al. Nature 465, 7298 (2010))

Linear chains + multiple oscillator modes

Mode frequencies: Be ions $f_x = 13.2$ MHz, $f_y = 14.2$ MHz

$f_z = 300$ kHz

$f_z = 1.5$ MHz



$$f_{\text{exchange}} = \frac{1}{2\pi} \frac{e^2}{2\pi\epsilon_0\omega_\alpha m_{\text{ion}} d^3}$$

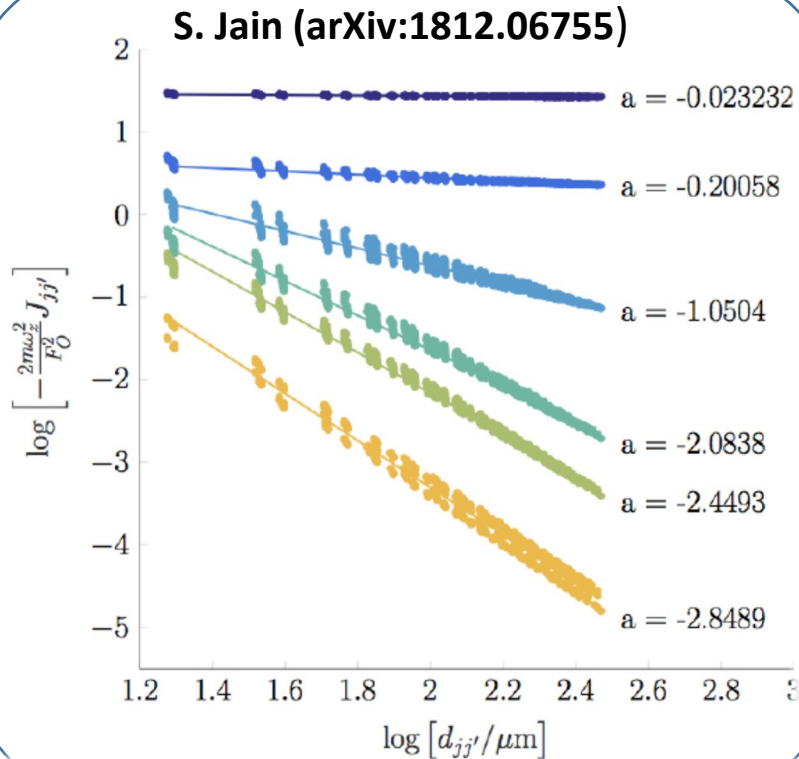
$$\hat{H}_{\text{ex}} = hf_{\text{exchange}} \left(\hat{a}^\dagger \hat{b} + \hat{a} \hat{b}^\dagger \right)$$

Distance between neighboring ions

Tuneable range spin-spin interactions

$$H_{\text{SPIN}} = \sum_{jj'} J_{jj'}(t) \sigma_j^z \sigma_{j'}^z$$

$$J_{jj'}^0 = \frac{E_O^2}{2\hbar} \sum_{\lambda} \frac{\omega_{\lambda}}{\mu_R^2 - \omega_{\lambda}^2} \text{Re}(\eta_{\lambda j}^* \eta_{\lambda j'})$$

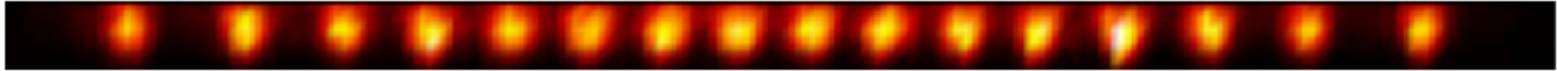


$$\frac{\mu_R - \omega_{\pm}}{2\pi} / \text{kHz}$$

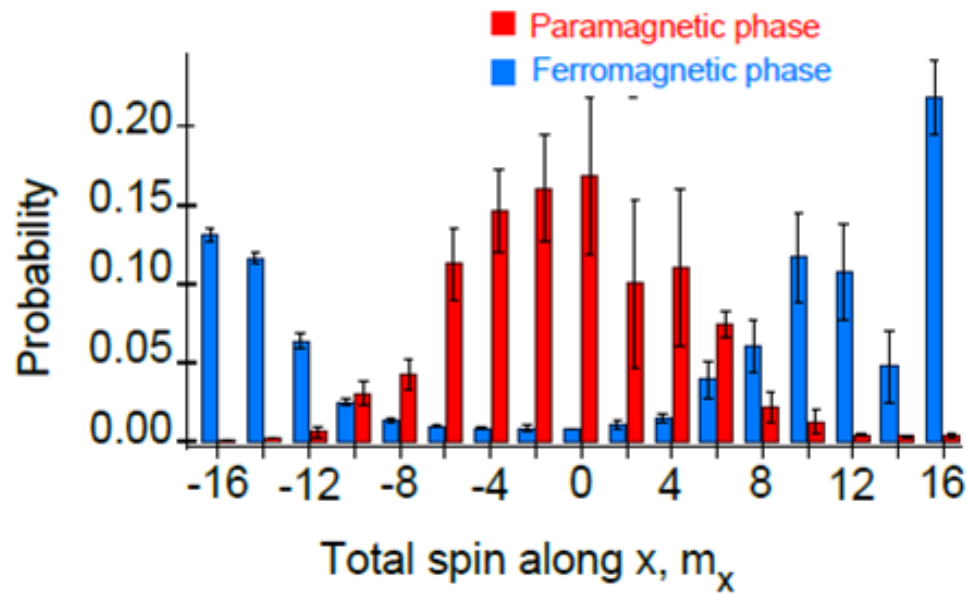
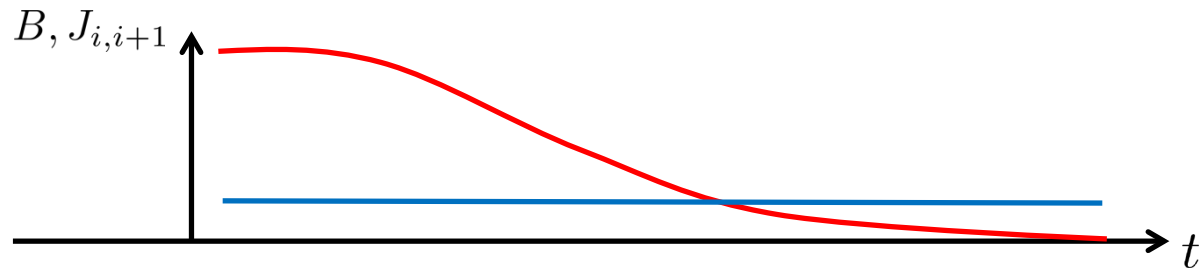
- 0.1
- 1
- 10
- 50
- 100
- 500

Quantum simulations in long ion strings

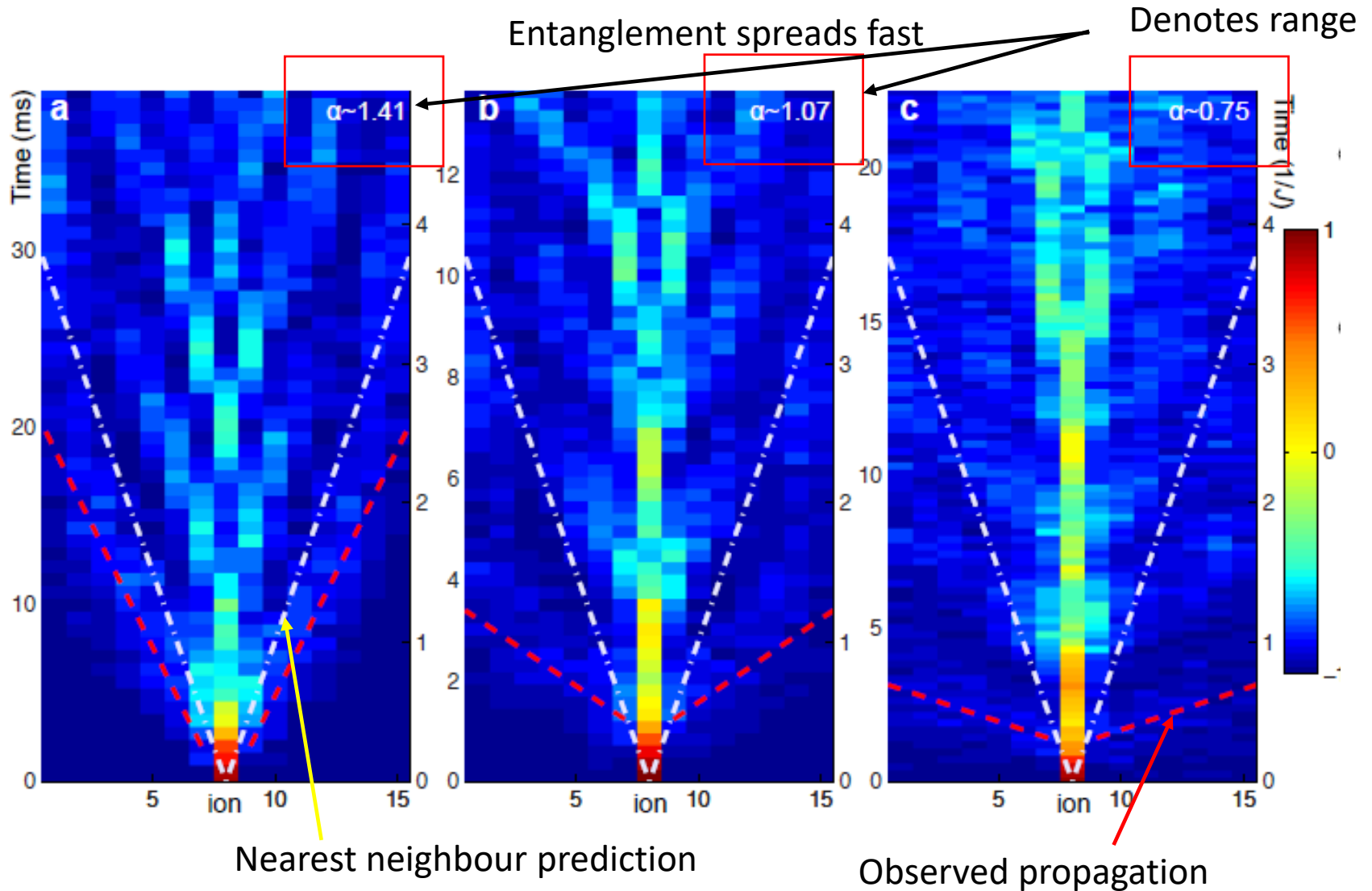
(up to 53 ions Zhang et al. Nature 2017)



$$\hat{H} = \sum_{j < i} J_{ij} \sigma_x^i \sigma_x^j - B \sum_i \sigma_y^i$$

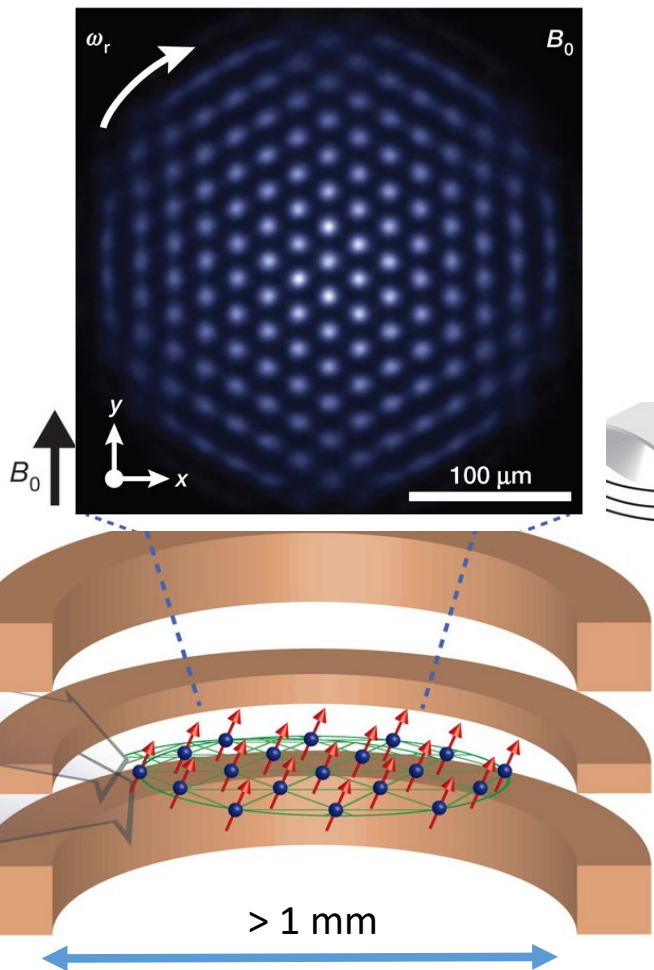


Tuneable range of interactions



2D ion crystals in macroscopic Penning traps

J. J. Bollinger, NIST



$$V_{\text{static}}(\mathbf{r}) + \{\mathbf{B}\}$$

Homogeneous magnetic field

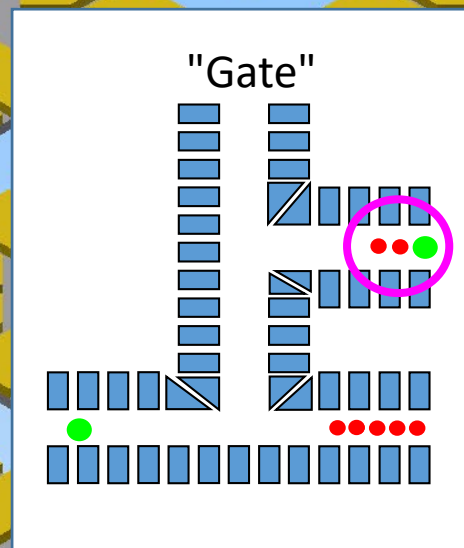
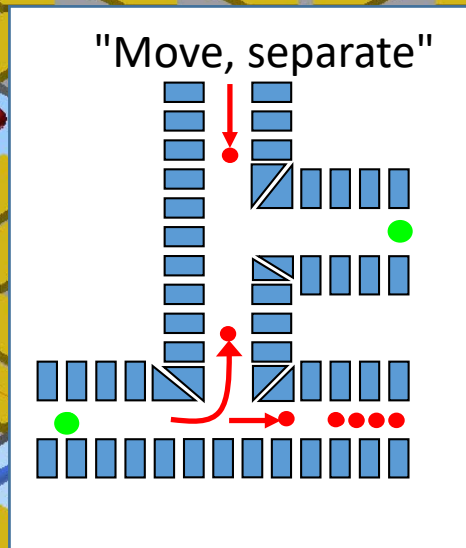
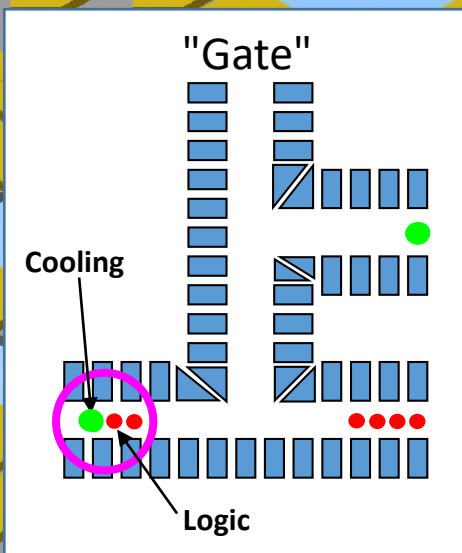
REPORT

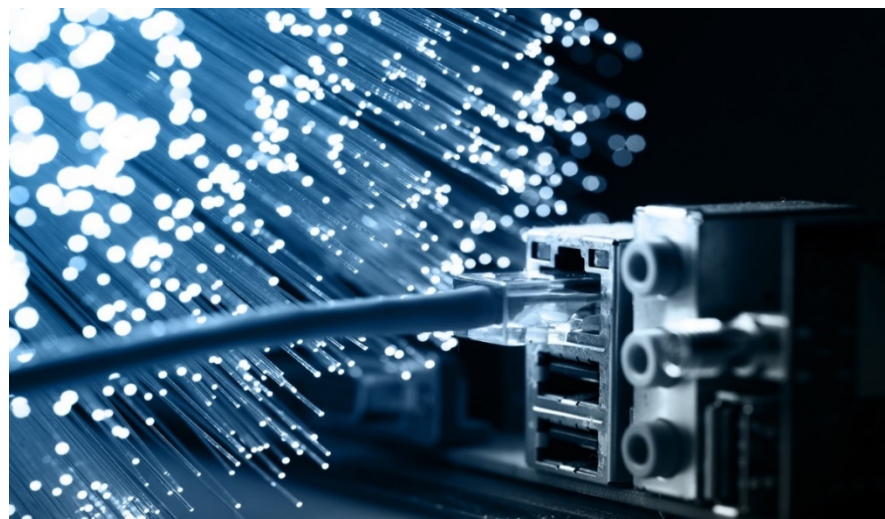
Quantum spin dynamics and entanglement generation with hundreds of trapped ions

Science 352, 6291 (2016)

The "Quantum CCD" architecture

Wineland et al., J. Res. N.I.S.T. (1998), Kielpinski et al. Nature 417, 709 (2002)



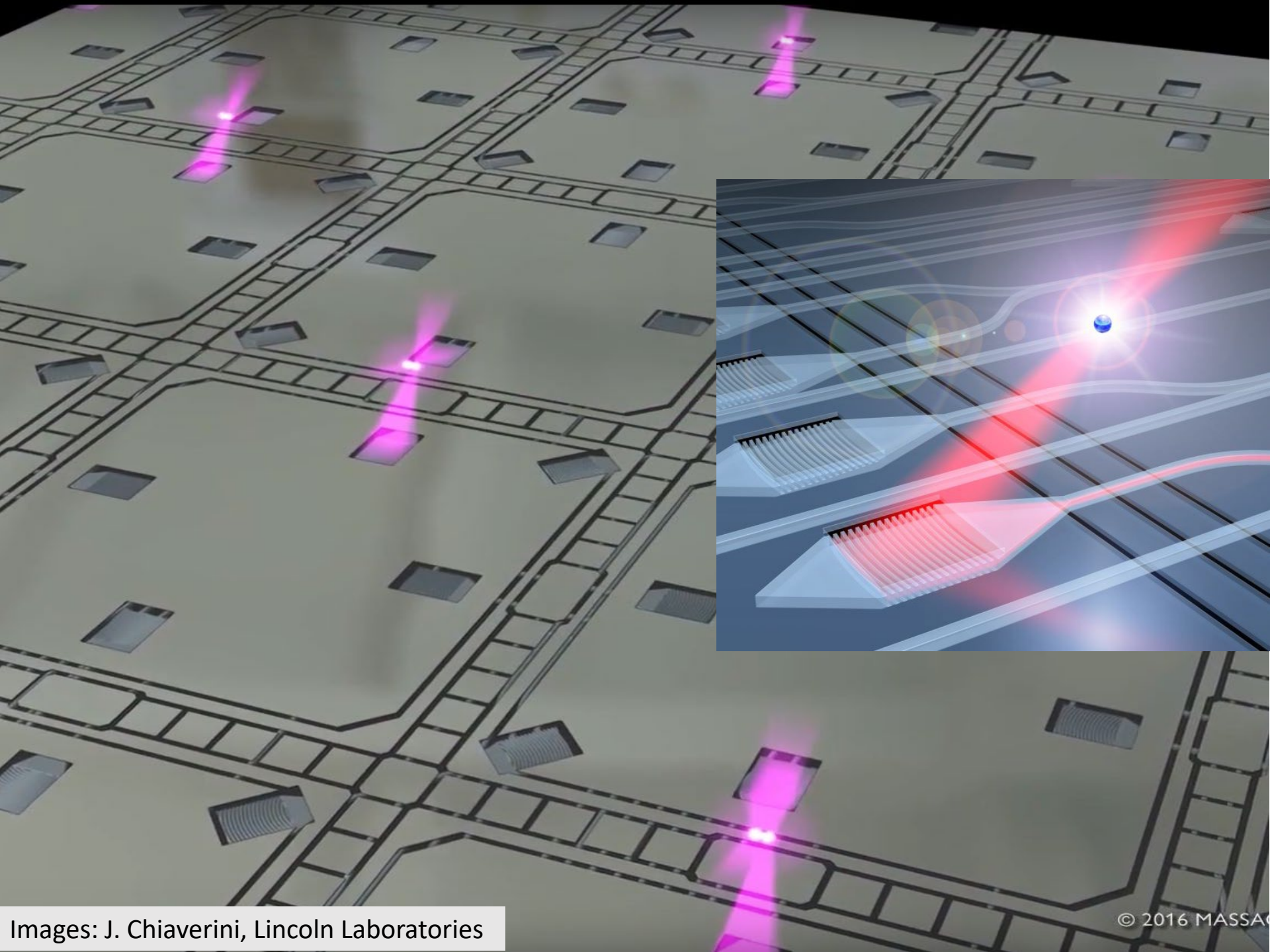


397 nm, 866 nm, 729 nm, 854 nm



On chip modulators
Input-output arrays
Plug and play fibre systems

Free-space bulky modulators (exceptions)
Self-developed UV fibres
Connectors home built



Images: J. Chiaverini, Lincoln Laboratories